American Diabetes Association. diabetes

Increased dihydroceramide/ceramide ratio mediated by defective expression of degs1 impairs adipocyte differentiation and function.

Journal:	*Diabetes*
Manuscript ID:	DB14-0359.R2
Manuscript Type:	Original Article
Date Submitted by the Author:	n/a
Complete List of Authors:	Barbarroja, Nuria; University of Cambridge, Wellcome Trust MRC Institute of Metabolic Science Rodriguez-Cuenca, Sergio; University of Cambridge, Wellcome Trust MRC Institute of Metabolic Science Nygren, Heli; VTT Technical Research Centre of Finland, Camargo, Antonio; Reina Sofia University Hospital, 4Lipids and Atherosclerosis Research Unit, IMIBIC Pirraco, Ana; University of Porto, Department of Biochemistry (U38-FCT), Faculty of Medicine Relat, Joana; Universitat de Barcelona, Departament de BioquímicaiBiologia Molecular Cuadrado, Irene; Universidad Complutense de Madrid, Departamento de Farmacología Pellegrinelli, Vanessa; University of Cambridge, Wellcome Trust MRC Institute of Metabolic Science Medina-Gomez, Gema; Universidad Rey Juan Carlos, Departamento de Bioquímica, Fisiología y Genética Molecular Lopez-Pedrera, Chary; Reina Sofia University Hospital, IMIBIC Tinahones, Francisco; Instituto de Salud Carlos III, Spain and Hospital Virgen de la Victoria, CIBER in Physiopathology of Obesity and Nutrition (CB06/03) Symons, David; University of Utah, Division of Endocrinology, Metabolism, and Diabetes Summers, Scott; Duke-National University of Singapore Graduate Medical School, Program in Cardiovascular and Metabolic Disorders Oresic, Matej; VTT Technical Research Centre of Finland, Vidal-Puig, Antonio; University of Cambridge, Clinical Biochemistry

Increased dihydroceramide/ceramide ratio mediated by defective expression of *degs1* impairs adipocyte differentiation and function.

Nuria Barbarroja[1,2]*, Sergio Rodriguez-Cuenca[1]*, Heli Nygren[3],Antonio Camargo[1,4],Ana Pirraco[1,5],Joana Relat[6], Irene Cuadrado[7], Vanessa Pellegrinelli[1], Gema Medina-Gomez[1,13],Chary Lopez-Pedrera[2],Francisco J. Tinahones[8],J. David Symons[9,10], Scott A. Summers[11],Matej Oresic[4,12]and Antonio Vidal-Puig[1,14]

***These two authors contributed equally to this work**

[1]Metabolic Research Laboratories, Wellcome Trust-MRC Institute of Metabolic Science, Addenbrooke's Hospital, University of Cambridge. Cambridge, UK.

[2]IMIBIC, Reina Sofia University Hospital, Cordoba, Spain.

[3]VTT Technical Research Centre of Finland, Espoo, Finland.

[4]Lipids and Atherosclerosis Research Unit, IMIBIC/Reina Sofia University Hospital, Spain.

[5]Department of Biochemistry (U38-FCT), Faculty of Medicine, University of Porto, Portugal.

[6]Departament de Bioquímica i Biologia Molecular, Universitat de Barcelona, 08028 Spain.

[7]Departamento de Farmacología, Universidad Complutense de Madrid, Spain.

[8]CIBER in Physiopathology of Obesity and Nutrition (CB06/03), Instituto de Salud Carlos III, Spain and Hospital Virgen de la Victoria, Malaga, Spain (IBIMA).

[9]College of Health, University of Utah, Salt Lake City, Utah.
[10]Division of Endocrinology, Metabolism, and Diabetes, University of Utah, Salt Lake City, Utah.
[11]Program in Cardiovascular and Metabolic Disorders, Duke-National University of Singapore Graduate Medical School, Singapore 169857

[12]Institute for Molecular Medicine Finland, Helsinki, Finland.

[13]Currently in Departamento de Bioquímica, Fisiología y Genética Molecular, Universidad Rey Juan Carlos, Spain.

[14]Wellcome Trust Sanger Institute, Hinxton, UK

Corresponding authors e-mail:

nuria.barbarroja.exts@juntadeandalucia.es;sr441@medschl.cam.ac.uk;ajv22@medschl.cam.ac.uk

Address reprint request to: Professor Antonio Vidal-Puig, Level 4, Institute of Metabolic Science, Box 289, Addenbrooke's Hospital, Cambridge, CB2 0QQ

Tel: 44-(0)1223762790 Fax: 44-(0)1223330598

RUNNING TITLE: *DEGS1*downregulation impairs adipocyte function.

Word count: 3997

Number of tables and figures: 7 figures and 1 table

ABSTRACT

Adipose tissue dysfunction is an important determinant of obesity-associated lipid induced metabolic complications. Ceramides are well known mediators of lipid induced insulin resistance in peripheral organs such as muscle. *DEGS1* is the desaturase catalysing the last step in the main ceramide biosynthetic pathway. Functional suppression of *DEGS1* activity results in substantial changes in ceramide species likely to affect fundamental biological functions such as oxidative stress, cell survival and proliferation. Here, we show that *degs1* expression is specifically decreased in the adipose tissue of obese patients and murine models of genetic and nutritional obesity. Moreover, loss of function experiments using pharmacological or genetic ablation of DEGS1 in preadipocytes prevented adipogenesis and decreased lipid accumulation. This was associated with elevated oxidative stress, cellular death and blockage of the cell cycle. These effects were **coupled** with increased dihydroceramide content. Finally, we validate *in vivo* that pharmacological inhibition of DEGS1 impairs adipocyte differentiation. These data identify *DEGS1* as a new potential target to restore adipose tissue function and prevent obesity-associated metabolic disturbances.

KEYWORDS: Adipocyte function, adipose tissue, *DEGS1*, obesity, insulin resistance and dihydroceramides

Dysfunction of white adipose tissue (WAT) and impaired differentiation of new adipocytes may lead to lipid leakage and inappropriate accumulation of ectopic lipids in peripheral organs, causing lipotoxicity and the Metabolic Syndrome(1). The toxic effects of lipids are determined by both the quantity and also by their qualitative characteristics(2). Whereas it is well documented that specific species of sphingolipids and ceramides mediate lipotoxicity in liver and muscle(3; 4), the contribution of specific lipotoxic species to WAT dysfunction in the context of obesity is still not well defined. It is known that in rodent WAT, ceramides increase in response to HFD(5; 6) concomitantly with the onset of insulin resistance(6). Lipid analysis of WAT from human obese subjects has produced conflicting results, showing either increased or decreased ceramide levels in obese and insulin resistant patients(7; 8).

Ceramides can be synthesised from sphingomyelins, but the main contributor to their biosynthesis is the *de novo* pathway. The final reaction of the *de novo* pathway is catalyzed by a Δ4-dihydroceramide desaturase (*DEGS1*) that adds a 4,5-trans-double bound on the sphingoid base of the dihydroceramide (DhCer) (9). The other enzyme, DEGS2 catalyzes the synthesis of phytoceramides(10), whose expression is restricted to skin, intestine and kidney.

There is evidence that downregulation of *degs1* increases the DhCer/Cer ratio in different cellular models. Although DhCer was considered an inactive precursor of ceramides(11), recent studies have suggested their relevance as modulators of cell cycle, apoptosis, autophagy or oxidative stress(12; 13), processes that *a priori* are expected to compromise the development and function of adipose tissue.

Since *DEGS1* is the key enzyme regulating the DhCer/Cer ratio, understanding its regulation is important in determining the pathophysiological relevance of this pathway in adipose tissue. Of note, degs1 has recently been identified in a GWAS study as a

candidate gene associated with fat mass accumulation in mice(14) further suggesting that *DEGS1* may be relevant for the adaptive accretion of adipose tissue. Moreover, *DEGS1* could be considered an attractive therapeutic target for obesity-associated insulin resistance, since Fenretinide has been claimed to improve insulin sensitivity *by inhibiting DEGS1*(15), although other molecular targets cannot be ruled out.

Here we show that *DEGS1* expression is selectively perturbed in the WAT of murine models of nutritional and genetically induced obesity and in WAT of morbidly obese patients. *In vitro* analysis revealed that both pharmacological inhibition and genetic ablation of DEGS1 results in impaired adipocyte differentiation and lipid accumulation, effects mediated by increased dihydroceramide content. In vivo, pharmacological inhibition of DEGS1 also resulted in impaired adipocyte differentiation. Decreased levels of DEGS1 were associated with increased oxidative stress, accelerated cellular death and blockage of cell cycle. We also show data supporting that *DEGS1* expression is regulated by PPARγ.

RESEARCH DESIGN AND METHODS

Mice husbandry

Animals were housed at 22-24°C with 12h light/dark cycles. Food and water were available *ad libitum*. Lean wildtype, PPARγ2$^{-/-}$ and PPARγ2$^{-/-}$xob/ob mice (POKO) (16) were used for profiling purposes. Mice were placed on a normal chow diet (D12450B) or in HFD (D12451) from Research Diets.

For the pharmacological inhibition of DEGS1, 10 weeks-old male C57BL/6 WT mice were used. Mice were given a HFD for 5weeks before C8-CPPC (Matreya) administration. All protocols used were approved by the UK Home Office.

Intraperitoneal injection of cyclopropenylceramide.

Mice were distributed in 2 groups (n=8) and administered daily vehicle (2-hydroxypropyl betacyclodextrine) or C8-CPPC (2mg/kg/day) for 9d via intraperitoneal injection. Mice were culled at the end of the experiment and WAT| was removed for **gene expression and** microscopy analysis. **No differences in food intake, lean mass and fat content were observed during the treatment.**

Ex vivo experiments in isolated mature adipocytes

Adipocytes from gonadal WAT of 16weeks C57BL/6 mice were obtained by collagenase type II digestion at 37ºC. After digestion, adipocytes were placed in DMEM media with or without 1µM C8-CPPC every 5h for a total period of 20h.

Retroviral Short Hairpin RNA Constructs for *DEGS1*

A RNAi-Ready pSIREN-RetroQ vectors (BD Biosciences) were used to target *degs1* in 3T3L1-cells. Sequences targeting *degs1* were ligated into the pSIREN vector as described in manufacturer's instructions. Retroviruses were generated by transfecting BOSC cells (ATCC) with the pSIREN plasmids using FuGene6 (Roche). Supernatant with the viral content was used to transfect 3T3-L1 preadipocytes. 24h after retroviral infection, the cells were selected with puromycin (4µg/ml).

Culture, differentiation and treatment of 3T3-L1 preadipocytes

Cells were differentiated into adipocytes (day9) accordingly to the protocol described in (17) with or without rosiglitazone 0.1µM. Lipid accumulation was assessed by Oil red O solution(18).

Pharmacological inhibition of *DEGS1* activity in vitro.

Effects on differentiation. At day 0 of differentiation, 3T3-L1 cells were treated with C8-CPPC 1µM and/or Rosiglitazone 0.1µM for 96h.

*Effects on lipolysis.*On day 8 of differentiation, after 48h treatment with C8-CPPC 1μM the cells were exposed to Noradrenaline (NA) (10^{-8} M and 10^{-7} M) for 6h.

Effects on insulin signalling. On day 8 of differentiation, after 48h treatment with C8-CPPC 1μM the cells were exposed to insulin (10nM and 100nM) for 15min.

Effects on glut4, adiponectin. On day 8 of differentiation, after 48h treatment with C8-CPPC 0.5-1μM the cells were exposed to insulin.

Effects on AMPK. On day 8 of differentiation, after 48h treatment with C8-CPPC 0.5-1μM the cells were exposed to insulin (10nM and 100nM), rosiglitazone (1nM and 10nM) and metformin (100nM) for 24h.

Dihydroceramide treatment.

3T3-L1 preadipocytes were treated at day 0 of differentiation with the induction cocktail and C2DhCer at 50μM for 3d, and a second batch of cells were exposed at day 3 of differentiation and treated with C2DhCer at 50μM for 3d. All batches were taken until final differentiation at day 9.

Human samples

The cohort included 28 morbidly obese (MO) and 6 non-obese subjects with no alterations to lipid or glucose metabolism, as controls (Table I). Approval for the study was given by the ethics committee and all patients gave their informed consent. Visceral adipose tissue biopsies were obtained from MO patients undergoing bariatric surgery (Scopinaro procedure) or laparoscopic surgery (hiatus hernia repair or cholecystectomies) for the lean subjects.

Western blotting

Protein extracts were prepared using the Nuclear and Cytoplasmic Extraction Reagents Kit (Pierce) according to manufacturer's instructions. Immunoblots were incubated with the following antibodies: PPARγ, C/EBPβ, CyclinA, (Santa Cruz) CyclinB1, D1, D3 and E1,cdk4, AKT, Ser473-pAKT, p44/42 MAPK, phospho-p44/42 MAPK, Ser660-pHSL, Ser565-pHSL, total HSL, ATGL, caveolin-1, plin1, glut4, adiponectin, and AMPK (Cell Signalling), adfp/adrp and abhd5 and anti-β-Actin (Abcam).

RT-PCR

RNA was extracted using TRI Reagent (Sigma) and reverse-transcribed to cDNA. Real-Time PCR using SYBRgreen was performed according to manufacturer's instructions (ABI). Primer sequences were obtained from Primer Blast(19). Expression of genes was corrected by the geometrical average of *18s*, β*2m*, *β-act*, and *36b4* using Bestkeeper (20).

Apoptosis: combined Annexin-V/propidium iodide staining

Viability was assessed by using an Annexin-V/propidium iodide kit (Bender MedSystems), according to manufacturer's recommendations. Binding of fluorescein-conjugated Annexin-V and propidium iodide was measured by FACSCalibur(BD).

Cellular proliferation:

Cell viability was assessed using an XTT colorimetric assay (Roche) following the protocol supplied by the manufacturer. Cell proliferation was analyzed by quantification of the incorporation of bromodeoxyuridine (Roche).

Bodipy staining, Reactive Oxygen Stress (ROS) production and mitochondrial content.

Cells were incubated with Bodipy at 4ºC or alternatively with 20µM DCF-DA or 100nM Mitotracker (Invitrogen) at 37°C for 30 min and analysed on a FACSCalibur.

Cellular oxygen consumption

Cells were exposed to oligomycin (1µM), C8-CPPC (0.9µM) and Antimycin/Rotenone (1µM each); O2 consumption was measured using the XF24 analyzer (Seahorse Bioscience) for a period of 90min.

Whole-mount confocal microscopy

Gonadal adipose tissue was fixed in 4% paraformaldehyde. Samples were incubated at 4°C with mouse pref-1 or rabbit Ki67 primary antibodies. Nuclei and neutral lipids were stained with Hoechst 33342, and BODIPY 493/503 respectively. Sample examination was performed using a Zeiss 510 confocal laser scanning microscope (Carl Zeiss). Pref1, Ki67, Bodipy positive cells and total cells (up to 913 cells/field) were automatically counted by using Image J software in 3 independent fields in each tissue.

Light microscopy analysis

Samples for adipose tissue H&E staining were prepared as described elsewhere (16). Adipocyte sizes were measured using Cell P (Olympus soft Imaging Solutions GMBH). Between 1000-3000 adipocytes from each mouse were used to obtain the mean cell-area.

Luciferase reporter assay

HEK293 cells were transfected using Lipofectamine LTX (Invitrogen), following the manufacturer's instructions. 75ng of the reporter plasmid (3xPPRE TKLuc) and 37.5ng

of the eukaryotic expression vector (pSV-PPARγ) were cotransfected to each well. The plasmid pRL-CMV (5ng/well) was included as an internal control. 24h post transfection cells were treated as indicated (DMSO, Rosiglitazone 10μM, GW1929 10μM, C2 and C16 DhCers and Cer 100 μM). Luciferase assays were performed using the dual luciferase reporter assay system (Promega).

Lipidomics

Cells were mixed with 0.9% NaCl and sonicated for 5 min at 5 ºC, 40 kHz. Samples were spiked with internal standard (IS). The samples were extracted with chloroform:methanol (2:1). The lower phase was collected and mixed with the labeled standard mixture (three stable isotope-labeled reference compounds). Lipid extracts were analyzed on a Q-ToF Premier mass spectrometer (Waters) combined with an Acquity Ultra Performance Liquid chromatography(UPLC/MS). The data was processed using MZmine software. The lipids were quantified by normalizing with corresponding IS.

Statistical analysis

Student t-test (unpaired), ANOVA and Duncan test were used for the statistical analysis. Statistically significance was set at $p<0.05$ and $p<0.01$. Spearman correlation was calculated to estimate the linear correlations between variables $p<0.01$.

RESULTS

DEGS 1 is downregulated in WAT in obese murine models.

Tissue distribution analysis showed that *degs1* is present in most tissues and it is particularly highly expressed in adipose tissue, liver and muscle, whereas *degs2* mRNA is only detected in intestine (Fig. 1A). *Degs1* expression *in vivo* was positively

correlated with WAT mass in lean healthy mice (Fig. 1B). However, this correlation was disrupted in murine models of nutritional and genetically induced obesity (HFD and ob/ob), where *degs1* mRNA expression was decreased vs. controls (Fig.1C and 1F). Of note, the dysregulation of *degs1* in obesity was limited to WAT, as its expression in liver or skeletal muscle was not affected in either HFD fed mice (Fig.1D and 1E) or in ob/ob mice (Fig.1G and H). DEGS1 was preferentially expressed in matured adipocytes vs. stromal vascular fraction (svf) in lean and ob/ob mice **(Fig.S1) and downregulated in ob/ob adipocytes vs lean adipocytes.** Moreover, this downregulation of *degs1* in total WAT of HFD fed and ob/ob mice was also recapitulated in visceral AT of morbidly obese patients (Fig S2A).

To determine whether the decrease in *degs1* expression was part of a global adaptation of *de novo* ceramide synthesis pathway in obesity, the expression of other genes in this pathway were measured. Expression of the *sptlc*1 and *sptlc*2 subunits were not changed in human visceral AT, nor in ob/ob WAT, but *sptlc*2 expression was increased in HFD WAT (Fig S2B-C). Moreover, both HFD and ob/ob **mouse** WAT exhibited a reduction in a subset of ceramide synthases, **suggests a possible** defect in the synthesis of specific **subset of** ceramides.

We then confirmed that modulators of obesity associated inflammation may contribute to the downregulation of *degs1,* as treatment of 3T3-L1 adipocytes with TNFα (5 ng/ml and 10ng/ml) for 48h resulted in a dose dependent downregulation of *degs1* mRNA expression (38.8±3.6% and 45.7±7.3% reduction respectively).

We then investigated a link between DEGS1 and the adipogenic programme. It is known that obese and insulin resistant murine models and humans have reduced expression of *pparγ2* in WAT. Furthermore we observed that expression of *pparγ2* and *degs1* were directly correlated in 3T3-L1 after treatment with Rosiglitazone (Fig.S3A).

To validate this *in vivo*, we analyzed the regulation of *degs1* in adipose tissue, liver and skeletal muscle of *pparγ2*KO and the POKO mice(16). WAT of *pparγ2*KO and POKO mice expressed significantly lower *degs1*mRNA levels vs. wt (Fig.S3B). This association was restricted to WAT since the expression of *degs1* in other metabolic organs such as skeletal muscle or liver was not affected when *pparγ2* was absent (Fig.S3C and D).

***DEGS1* controls important cellular functions such as proliferation, survival and oxidative stress in 3T3-L1 adipocytes.**

A stable *degs1* knock-down 3T3-L1 cell line (65%) (Fig.2A) resulted in inhibition of cell growth after 24h (Fig.2B-C). *Degs1* knock-down also induced cell death (13.7%) and apoptosis (6.3%)(Fig.2E). These were associated with a decrease in cyclin-A and cdk2 in *degs1*KD proliferating cells (Fig.2F) as well as elevated Bax and caspase-3mRNA (Fig.2D). Elevated reactive oxygen species (ROS) production **(Fig.2I) along with an upregulation of the expression of antioxidant genes was observed** in *degs1*KD preadipocytes (Fig.2H). This was accompanied by impaired mitochondrial oxygen consumption (Fig.2G) without changes in the **number** of mitochondria (Fig.2J).

***DEGS1* is required for adipocyte differentiation.**

Expression of *degs1* is increased during **normal** differentiation of 3T3-L1 adipocytes (Fig.3A). To investigate whether ablation of *DEGS1* affected adipogenesis, 3T3-L1 *degs1*KD cells were induced to differentiate. At d9, *degs1KD cells* showed impaired lipid accumulation **vs. controls** (Fig.3B). Moreover, *pref1* mRNA expression, a marker for preadipocytes was not decreased in *degs1*KD cells at d9 suggesting that a relevant number of cells remained in the preadipocyte stage (Fig.3C). In addition, expression of

proadipogenic and lipogenic genes were downregulated (Fig.3D). Interestingly, treatment with rosiglitazone only partially improved the differentiation and lipid accumulation rates of *degs1*KD cells (Fig. S4A-**B**).

We tested whether *DEGS1* expression may affect the mitotic clonal expansion (MCE). **In *degs1*KD cells,** *pparγ* and *cebpβ* were downregulated compared to controls at time 0 and 24h following differentiation induction (Fig. S5AB). The expression of *PPARγ* and several cyclins involved in adipogenesis were measured at earlier time points. We noted a strong effect of *degs1* **depletion** on PPARγ2 mRNA from time 0. Additionally**, reduced levels of** *degs1* blocked MCE as indicated by the inhibition of cyclin D1 and cdk2 expression between time 0 and **4h** hours after the induction (Fig. S5AB). Cyclin E and cyclin D3 expression was also inhibited but at later time points.

Pharmacological inhibition of *DEGS1* recapitulates *DEGS1KD* antiadipogenic phenotype.

Use of C8-cyclopropenylceramide (C8-CPPC), a selective inhibitor of *DEGS1*(21) further confirmed the **relevance of DEGS1 in adipogenesis**. Similarly to degs1KD cells, 3T3-L1 cells were induced to differentiate and treated **simultaneously** with C8-CPPC from time 0h every 6h for 48h. C8-CPPC decreased the expression of proadipogenic transcription factors such as PPARγ and C/EBPβ as well as lipogenic genes (Fig. 4AC). The antiadipogenic effect of C8-CPPC persisted after Rosiglitazone treatment (Fig. 4AC). As expected, analysis of neutral lipids showed that 3T3-L1 cells treated with C8-CPPC for 96h accumulated significantly less lipids compared to untreated cells (Fig. 4D).

Pharmacological inhibition of DEGS1 also impairs adipocyte differentiation *in vivo.* We administered C8-CPPC IP to mice fed a HFD for 5weeks, an experimental protocol known to trigger adipocyte hyperplasia. Molecular analysis of the WAT from mice treated with C8-CPPC presented higher levels of pref-1+ cells, suggesting an increase in the number of preadipocytes vs. controls. Interestingly, a significant number of preadipocytes **showed evidence of increased** proliferation (Ki67+) whereas the number of differentiating preadipocytes (pref1+, bodipy +) was significantly smaller in comparison to controls (Fig.5A). These data were reinforced at mRNA level by showing increased expression of pref-1 and gata2 (Fig 5B) and the presence of less smaller adipocytes in treated mice (Fig.S6). Altogether, these data suggest C8-CPPC mediated inhibition of DEGS1 impaired the capacity of preadipocytes to differentiate into adipocytes *in vivo*.

DEGS1 is required for lipid accumulation, basal lipolysis and glucose uptake in mature adipocytes.

We next focused on the effects of DEGS1 inhibition in fully differentiated adipocytes **by treating isolated** mature adipocytes-from the gonadal adipose tissue of C57BL/6 mice- with C8-CPPC for 24h. C8-CPPC caused a decrease in the expression of lipid metabolism genes as well as an increase in antioxidant genes **(Fig S7)** recapitulating our observations in **3T3L1** preadipocytes.

We further investigated the effects of inhibiting DEGS1 **on** lipolytic **activity** and insulin signalling, and measured adiponectin expression as a representative fingerprint of global adipocyte homeostasis **in mature differentiated 3T3L1 adipocytes**. Thus, we observed that basal lipolytic activity was decreased in mature differentiated 3T3L1 adipocytes

when treated with C8-CPPC in non-stimulated conditions (Fig. 6A). Systematic evaluation of the lipolytic axis showed that under basal conditions**, phosphorylation of Ser565 was also substantially increased by C8-CPPC concomitantly with a minor downregulation of Ser660 phosphorylation (Fig.6B-D) suggesting a decreased HSL activity. Moreover, total levels of HSL were also decreased in C8-CPPC treated cells.** These data suggest that pharmacological inhibition of DEGS1 in mature adipocytes disrupts the lipolytic response under non-stimulated conditions a defect that was superseded in the presence of NA.

Finally we characterised the effects of **pharmacological** inhibition of DEGS1 on insulin signalling in 3T3-L1 mature adipocytes treated with C8-CPPC for 48h as described above, and subsequently incubated in the presence of increasing doses of insulin. No major differences where observed in **the phosphorylation of AKT** in C8-CPPC treated cells after acute insulin stimulation (Fig.6E). However, we found that Glut4 protein levels were increased in C8-CPPC treated cells, suggesting that glucose uptake may be increased (Fig.6F). Interestingly, we also did not observe any differences in either adiponectin levels in response to C8-CPPC or in AMPK phosphorylation, a known inducer of adiponectin, although increased levels of tAMPK were observed (Fig 6GH).

Both, Pharmacological and Genetic inhibition of *DEGS1* increases dihydroceramide/ceramide ratio in 3T3-L1-cells.

We confirmed that C8-CPPC increased the DhCer/Cer ratio in 3T3L-1 preadipocytes upon inhibition of *DEGS1* (Fig.4E). Similarly, *degs1*KD preadipocytes (d0) exhibited an increased DhCer/Cer ratio vs. controls. Downregulation of *degs1* expression in *degs1*KD cells was accompanied by a dowregulation of serine palmitoyltransferase

(*sptlc*1) and Ceramide synthase 6 (*Cers*6), suggestive of a homeostatic readjustment of the biosynthetic pathway to compensate for the dysfunction of degs1. Other genes related to ceramide homeostasis such as neutral ceramidase (*ncdase*), and glycosylceramide synthase (*gcs*) were also downregulated.

Curiously, at d9, *degs1*KD cells, **despite impaired differentiation**, showed a complete restoration of the DhCer/Cer ratio (indicated by the normalization of the ceramide pool) (Fig.S8A). This could be partially explained by a compensation mechanism, mediated by downregulation of neutral ceramidases and the conversion of sphyngomyelins to ceramides (upregulation of sphyngomyelinase 2) (Fig.S8B).

The Impairment of adipocyte differentiation during early adipogenesis by DEGS1 inhibition is recapitulated by Dihydroceramides per se.

We finally sought to validate whether DhCer by itself could mediate the effects of DEGS1 inhibition on adipocyte differentiation in our models of genetic or pharmacological inhibition of degs1. 3T3-L1cells were treated with C2-DhCer during a) the MCE at time 0 and b) at day 3 after differentiation. DhCer inhibited lipid accumulation (Fig.7A) and the expression of genes involved during the early stages of adipogenesis (Fig. 7B).

Since synthetic sphingolipid analogues are known to modulate PPARs activity(22), we investigated whether both C2 and C16 DhCer could exert a repressive effect on PPARγ activation in the presence of the PPARγ ligands (Fig. 7C). Our results show that DhCer can also block the ligand-mediated transactivation of PPARγ. Similar results were obtained with ceramides, indicating these effects were not a consequence of the unsaturation of the sphingoid moiety (data not shown).

DISCUSSION

The DhCer/Cer ratio has an important homeostatic regulatory role in the cell, contributing to cell survival, autophagy and oxidative stress(12; 13). Here we identify DEGS1 as an essential metabolic enzyme which is dysregulated in obese states and contributes to adipose tissue dysfunction. Our complementary *in vitro* and *in vivo* approaches reveal that reduced DEGS1 function impairs adipogenesis and lipogenesis **programmes** and increases oxidative stress.

DEGS1 is expressed in WAT and correlates **in rodents** with fat mass in healthy states, an association that is disrupted in severe forms of obesity. Expression of *DEGS1* in liver or muscle is not affected by obesity, further indicating that the WAT is particularly susceptible to changes in ceramide metabolism in obese states. The relevance to human obesity is confirmed by the downregulation of *DEGS1* in the adipose tissue of morbidly obese patients, and by recent reports showing that DhCer rather than Cer content positively correlates with BMI and waist circumference in cohorts of overweight-obese subjects(23; 24). To date, only a single functional mutation in the *Degs1*gene has been reported in humans **where patients demonstrate** increased serum DhCer and decreased cholesterol esters, and decreased waist to hip ratio(25). Globally considered, these data suggest the existence of an association between *DEGS1* function and fat mass.

The molecular mechanism leading to the defective adipose tissue expression of *degs1* in human and rodent obesity is unknown. Here, we have shown that TNFα, a mediator of obesity induced inflammation and insulin resistance, decreases the transcriptional expression of *degs1* in cultured adipocytes, which suggests that low chronic inflammation may contribute to *DEGS1* dysfunction. Other obesity associated processes, such as increased oxidative stress and hypoxia, have been shown to impair *DEGS1* activity and increase DhCer levels(26). Our results also show a positive

association between levels of the proadipogenic *pparγ2* isoform and *degs1* in adipose tissue, and given the documented downregulation of *pparγ2* in adipose tissue in obese insulin resistant states, it is conceivable that decreased levels of *pparγ2* may contribute to the defective expression of *degs1* associated to obesity.

Studies in rodents have shown that Cer are increased in the WAT of animals fed HFD(5) concomitantly with the onset of insulin resistance(6). Results from ob/ob mice and human obese studies are more unclear, where both increased or decreased levels of ceramides have been reported(7; 8). This suggests that Cer synthesis may be dependent on the severity of the obese state and the strength of the adaptive homeostatic responses attempting to restore their normal balance.

Our pharmacological **and gene ablation** studies have shown that inhibition of *DEGS1* is associated with oxidative stress, cellular death, impaired **adipocyte differentiation, impaired** lipid accumulation and **impaired** basal lipolysis in mature adipocytes.

Our *in vitro* studies revealed that the **defect in adipogenesis programme caused by depletion of** *DEGS1* occurs **during** the early stages of adipogenesis **(MCE)** when PPARγ controls the expression of genes that regulate the cell cycle, by directly interacting with cyclin D3. Another cyclin involved in adipocyte differentiation is cyclin D1, and here we show that downregulation of *DEGS1* blocks PPARγ activity and cyclins such as D1, D3, E, as well as decreasing cdk2, which modulates PPARγ activity during adipogenesis. **These data are consistent with studies showing that downregulation of *degs1* by siRNA inhibits cell growth and arrests the cell cycle in cancer cells(12), and where its overexpression increased cell migration and metastasis(27).**

The pharmacological inhibition of DEGS1 in vivo validated the results obtained in vitro and strengthen the concept that functional *degs1* is required for the full differentiation of preadipocytes into mature adipocytes.

We also provide evidence that both pharmacological and genetic ablation of *degs1* **certainly increased** DhCer levels in in vitro models which according to our results **in in vitro models** may directly block adipocyte differentiation and lipid deposition. This effect on lipid accumulation was more severe when the treatment was administered during the first three days of differentiation, suggesting a direct impact of DhCer accumulation during early stages of adipogenesis. **We also provide evidence showing that a**ccumulation of DhCers can also directly repress the transcriptional activity of PPARγ and hence **could contribute to** impair the capacity of the preadipocytes to develop a full adipogenic programme.

These observations strengthen the concept that DhCers are not merely inert precursors of ceramides. Nevertheless, the molecular mechanism linking DhCers accumulation and dysregulation of the cell cycle and other cellular events remains elusive. One possible mechanism is that changes in the DhCer/Cer ratio may disrupt membrane dependent structures by altering the levels of cholesterol and/or caveolin in lipid rafts, which are known to be highly sensitive to sphingomyelin **pool**. Alternatively, **changes in the DhCer/Cer ratio** may disturb the global phospholipidome, potentially altering membrane-associated processes relevant to adipocyte function. These are important questions to address in future research.

In summary, our results indicate that defects in DEGS1 in the context of the MetS may compromise adipose tissue expansion and function through the combined inhibition of adipogenesis, promotion of cell death and oxidative stress due to the direct

accumulation of DhCers. Thus, our data suggests that the selective manipulation of *DEGS1* and/or its substrates in WAT may be a pathophysiologically advantageous strategy to improve adipose tissue homeostasis and ameliorate the burden of obesity associated metabolic complications.

ACKNOWLEDGMENTS

We thank Dr. Carobbio Mrs. Peirce and Ms. Philips (Wellcome Trust-MRC IMS, University of Cambridge, UK) for their excellent technical advice, support and suggestions. This work was funded by Medical Research Council, MDU MRC, FP7-ETHERPATHS and the British Heart Foundation (BHF). We declare no conflict of interest.

NB and SRC, AC, JRP, AP, ICB, VP, GMG and CLP performed the *in vitro and ex vivo* experiments, collected and analyzed the data. HN and MO developed analytical platforms and performed and analysed lipidomic experiments. NB, FJT held and characterized the human cohorts, collected gene expression data from adipose depots, and analyzed the data. NB, SRC, AJS, SS and AVP designed the experiments. NB, SRC, HN, AC, JRP, AP, ICB, VP, GMG, CLP, FJT, AJS, SS, MO and AVP discussed the manuscript. NB, SRC and AVP coordinated and directed the project. NB, SRC and AVP developed the hypothesis and wrote the manuscript.

REFERENCES

1. Montague CT, O'Rahilly S: The perils of portliness: causes and consequences of visceral adiposity. Diabetes 2000;49:883-888
2. Carobbio S, Rodriguez-Cuenca S, Vidal-Puig A: Origins of metabolic complications in obesity: ectopic fat accumulation. The importance of the qualitative aspect of lipotoxicity. Curr Opin Clin Nutr Metab Care 2011;14:520-526
3. Chavez JA, Summers SA: Lipid oversupply, selective insulin resistance, and lipotoxicity: molecular mechanisms. Biochim Biophys Acta 2010;1801:252-265
4. Chavez JA, Summers SA: A ceramide-centric view of insulin resistance. Cell Metab 2012;15:585-594
5. Shah C, Yang G, Lee I, Bielawski J, Hannun YA, Samad F: Protection from high fat diet-induced increase in ceramide in mice lacking plasminogen activator inhibitor 1. J Biol Chem 2008;283:13538-13548
6. Turner N, Kowalski GM, Leslie SJ, Risis S, Yang C, Lee-Young RS, Babb JR, Meikle PJ, Lancaster GI, Henstridge DC, White PJ, Kraegen EW, Marette A, Cooney GJ, Febbraio MA, Bruce CR: Distinct patterns of tissue-specific lipid accumulation during the induction of insulin resistance in mice by high-fat feeding. Diabetologia 2013;56:1638-1648
7. Blachnio-Zabielska AU, Koutsari C, Tchkonia T, Jensen MD: Sphingolipid content of human adipose tissue: relationship to adiponectin and insulin resistance. Obesity (Silver Spring) 2012;20:2341-2347
8. Blachnio-Zabielska AU, Pulka M, Baranowski M, Nikolajuk A, Zabielski P, Gorska M, Gorski J: Ceramide metabolism is affected by obesity and diabetes in human adipose tissue. J Cell Physiol 2012;227:550-557
9. Ternes P, Franke S, Zahringer U, Sperling P, Heinz E: Identification and characterization of a sphingolipid delta 4-desaturase family. J Biol Chem 2002;277:25512-25518
10. Mizutani Y, Kihara A, Igarashi Y: Identification of the human sphingolipid C4-hydroxylase, hDES2, and its up-regulation during keratinocyte differentiation. FEBS Lett 2004;563:93-97
11. Ahn EH, Schroeder JJ: Induction of apoptosis by sphingosine, sphinganine, and C(2)-ceramide in human colon cancer cells, but not by C(2)-dihydroceramide. Anticancer Res 2010;30:2881-2884
12. Kraveka JM, Li L, Szulc ZM, Bielawski J, Ogretmen B, Hannun YA, Obeid LM, Bielawska A: Involvement of dihydroceramide desaturase in cell cycle progression in human neuroblastoma cells. J Biol Chem 2007;282:16718-16728
13. Siddique MM, Li Y, Wang L, Ching J, Mal M, Ilkayeva O, Wu YJ, Bay BH, Summers SA: Ablation of dihydroceramide desaturase 1, a therapeutic target for the treatment of metabolic diseases, simultaneously stimulates anabolic and catabolic signaling. Mol Cell Biol 2013;33:2353-2369
14. Parks BW, Nam E, Org E, Kostem E, Norheim F, Hui ST, Pan C, Civelek M, Rau CD, Bennett BJ, Mehrabian M, Ursell LK, He A, Castellani LW, Zinker B, Kirby M, Drake TA, Drevon CA, Knight R, Gargalovic P, Kirchgessner T, Eskin E, Lusis AJ: Genetic control of obesity and gut microbiota composition in response to high-fat, high-sucrose diet in mice. Cell Metab 2013;17:141-152
15. Bikman BT, Guan Y, Shui G, Siddique MM, Holland WL, Kim JY, Fabrias G, Wenk MR, Summers SA: Fenretinide prevents lipid-induced insulin resistance by blocking ceramide biosynthesis. J Biol Chem 2012;287:17426-17437
16. Medina-Gomez G, Gray SL, Yetukuri L, Shimomura K, Virtue S, Campbell M, Curtis RK, Jimenez-Linan M, Blount M, Yeo GS, Lopez M, Seppanen-Laakso T,

Ashcroft FM, Oresic M, Vidal-Puig A: PPAR gamma 2 prevents lipotoxicity by controlling adipose tissue expandability and peripheral lipid metabolism. PLoS Genet 2007;3:e64
17. Roberts LD, Virtue S, Vidal-Puig A, Nicholls AW, Griffin JL: Metabolic phenotyping of a model of adipocyte differentiation. Physiol Genomics 2009;39:109-119
18. Ramirez-Zacarias JL, Castro-Munozledo F, Kuri-Harcuch W: Quantitation of adipose conversion and triglycerides by staining intracytoplasmic lipids with Oil red O. Histochemistry 1992;97:493-497
19. Ye J, Coulouris G, Zaretskaya I, Cutcutache I, Rozen S, Madden TL: Primer-BLAST: a tool to design target-specific primers for polymerase chain reaction. BMC Bioinformatics 2012;13:134
20. Pfaffl MW, Tichopad A, Prgomet C, Neuvians TP: Determination of stable housekeeping genes, differentially regulated target genes and sample integrity: BestKeeper--Excel-based tool using pair-wise correlations. Biotechnol Lett 2004;26:509-515
21. Triola G, Fabrias G, Llebaria A: Synthesis of a Cyclopropene Analogue of Ceramide, a Potent Inhibitor of Dihydroceramide Desaturase. Angew Chem Int Ed Engl 2001;40:1960-1962
22. Tsuji K, Satoh S, Mitsutake S, Murakami I, Park JJ, Li Q, Chang YT, Chung SK, Igarashi Y: Evaluation of synthetic sphingolipid analogs as ligands for peroxisome proliferator-activated receptors. Bioorg Med Chem Lett 2009;19:1643-1646
23. Mamtani M, Meikle PJ, Kulkarni H, Weir JM, Barlow CK, Jowett JB, Bellis C, Dyer TD, Almasy L, Mahaney MC, Duggirala R, Comuzzie AG, Blangero J, Curran JE: Plasma dihydroceramide species associate with waist circumference in Mexican American families. Obesity (Silver Spring) **2014 Mar;22(3):950-6.**
24. Weir JM, Wong G, Barlow CK, Greeve MA, Kowalczyk A, Almasy L, Comuzzie AG, Mahaney MC, Jowett JB, Shaw J, Curran JE, Blangero J, Meikle PJ: Plasma lipid profiling in a large population-based cohort. J Lipid Res 2013;54:2898-2908
25. Curran J, Meikle P, Weir J, Jowett J. Deep Sequencing in Extended Pedigrees Reveals a Major Rare Non-Synonymous Variant Influencing the De Novo Ceramide Synthesis Pathway. Abstract presented in *American Society of Human Genetics meeting*. Boston, 2013.
26. Idkowiak-Baldys J, Takemoto JY, Grilley MM: Structure-function studies of yeast C-4 sphingolipid long chain base hydroxylase. Biochim Biophys Acta 2003;1618:17-24
27. Zhou W, Ye XL, Sun ZJ, Ji XD, Chen HX, Xie D: Overexpression of degenerative spermatocyte homolog 1 up-regulates the expression of cyclin D1 and enhances metastatic efficiency in esophageal carcinoma Eca109 cells. Mol Carcinog 2009;48:886-894

FIGURE LEGENDS

FIG.1.(A)Tissue distribution of degs1 (B) Correlation of degs1 mRNA expression and fat pad size. The Spearman correlation coefficients were calculated to estimate the linear correlations between variables. The rejection level for a null hypothesis was $p < 0.01$. Data from 14 lean mice (C-E) Expression levels of *degs1* mRNA in response to HFD (F-H)Expression levels of *degs1* mRNA in ob/ob mice. Mean ± Sem for 6 to 8 animals per group. *$p<0.05$ vs. wt. WAT, white adipose tissue; BAT, brown adipose tissue; **SKM, skeletal muscle:** HFD, High fat diet; WT, wild type; IngFat; Inguinal Fat; gWAT; gonadal white adipose tissue.

FIG.2(A)mRNA expression of *degs1* in 3T3-L1 treated with shRNA against *degs1*(B and C)Cell proliferation (XTT and BrdU assays every 24h until 96h **and 72h respectively**)(D) mRNA expression of *Cdk2, Bcl2, Bax* and *Caspase3*. (E) Apoptosis and cell death rate (F) Protein expression of Cdk2 (G) Oxygen consumption rate (OCR) (H)mRNA expression of antioxidant machinery genes. (I)Reactive oxidative species production (ROS)(J)Mitochondria levels. **All these experiments were perfomed in degs1KD and wild type 3T3-L1 cells**. Mean±Sem of three separate experiments performed in triplicate; *$p< 0.05$.

FIG.3.(A)mRNA expression of degs1 in 3T3-L1 cells during adipocyte differentiation.(B)Lipid accumulation at d9 of differentiation, Oil Red O Staining (C) mRNA expression of PREF1 in wild type and degs1 KD cells during differentiation. (D)mRNA expression of genes involved in adipocyte differentiation and lipid accumulation. Mean±Sem of three separate experiments performed in triplicate; *$p< 0.05$.

FIG.4. 3T3-L1 cells treated with C8-CPPC and/or Rosiglitazone (A and B) mRNA expression of genes involved in adipocyte differentiation and lipid accumulation at 24 and 48h after induction. (C) Protein expression levels of PPARγ2 and cEBPα (D) Lipid content after 48 and 96h of differentiation. Mean ± Sem of two separate experiments performed in triplicate. One way ANOVA was used to analyze statistical significance between treatments at 24 h and 48 h. Significant differences (Duncan; $p<0.05$) are indicated with different words. (E) Dihydroceramide and ceramide levels after 48h of differentiation. Mean ± Sem of two separate experiments performed in triplicate $p<0.05$.

FIG.5. C8-CCP inhibitor increases proliferation and decreases lipid accumulation in preadipocytes *in vivo***.** 10 weeks old mice were given a 45% HF diet for 5 weeks before treated intraperitoneally with vehicle or C8-CCP inhibitor (2mg/kg/day) during 9 days. (A) Representative images of immunofluorescence analysis of gonadal adipose tissue of control (vehicle) and C8-CCP-treated mice are presented with Pref-1 (*Cyan*) and ki-67 (*red, white arrows*). Nuclei and lipids are respectively stained with Hoechst (*blue*) and Bodipy (*green*). Scale bar 100 or 20 µm. Quantification of preadipocytes (left graph, % Pref-1 positive cells/total cells) and Ki67 (white bars) /Bodipy (dark grey bars) positive cells among preadipocytes (Pref-1 positive cells, grey bars). (B) mRNA expression of preadipocyte markers and pparg, desg1, adiponectin, caspase 3 and fas in gonadal adipose tissue of control and C8-CCP-treated mice. n=7-8 mice per experimental group; mean±SEM;*$p<0.05$, ***$p<0.0001$ versus vehicle

FIG.6. (A) Glycerol release in 3T3-L1 adipocytes exposed 48h with C8-CPPC and stimulated with nor-adrenalin (NA) for 6h. (B-D) Results from Western blot analysis for p-HSL/HSL ratio and total HSL in 3T3L1 adipocytes exposed 48h with C8-CPPC and

stimulated with NA for 6h. Graphs show the mean ± SEM of two separated experiments; $p< 0.05$, $^{\&}p<0.05$ vs cells without NA and $^{\#}p<0.05$ vs cells without NA or treated with 10^{-8}M NA. (E) Effects of pharmacological inhibition of DEGS1 on insulin signalling. Results from Western blot analysis for p-AKT and AKT in 3T3-L1 adipocytes exposed 48h or 72h with C8-CPPC 1µM and increased concentrations of Insulin (10 nM-100 nM) for 15min. (F and G9) Results from Western blot analysis for Glut4 and adiponectin in 3T3-L1 adipocytes exposed with C8-CPPC 0.5-1µM and Insulin (100 nM) for 48 hours. (H) Results from Western blot analysis for AMPK in 3T3-L1 adipocytes exposed with C8-CPPC 0.5-1µM and insulin (100nM), rosiglitazone (1 nM) and metformin (100 nM) for 48 hours. $^{b}p< 0.05$ versus untreated cells (Insulin, Rosi or Metformin effect) and; $^{b}p< 0.05$ versus 0 µM C8-CPPC (C8-CPPC effect)

FIG.7. (A and B) Dihydroceramides impair adipocyte differentiation during early adipogenesis. 3T3L1 preadipocytes treated withC2-DhC (50µM) for a period of 48h at d0 or at d3 of differentiation. ORO staining and mRNA expression of adipogenesis and lipid metabolism genes. Mean ± Sem of two separated experiments performed in triplicate; $*p< 0.05$ vs. control. (C) Dihydroceramides decrease ligand-mediated PPARγ transactivation. Cells were treated with DMSO as a control group, Rosiglitazone 10uM, GW1929 10uM, C2 and C16 dihydroceramides and ceramides 100 uM as indicated. Graphs represent the average of 3 independent experiments. $p< 0.05$. **(*) vs control cells, (#) vs Rosiglitazone and (&) vs GW1929.**

Increased dihydroceramide/ceramide ratio mediated by defective expression of *degs1* impairs adipocyte differentiation and function.

Nuria Barbarroja[1,2]*, Sergio Rodriguez-Cuenca[1]*, Heli Nygren[3],Antonio Camargo[1,4],Ana Pirraco[1,5],Joana Relat[6], Irene Cuadrado[7], Vanessa Pellegrinelli[1], Gema Medina-Gomez[1,13],Chary Lopez-Pedrera[2],Francisco J. Tinahones[8],J. David Symons[9,10], Scott A. Summers[11],Matej Oresic[4,12]and Antonio Vidal-Puig[1,14]

***These two authors contributed equally to this work**

[1]Metabolic Research Laboratories, Wellcome Trust-MRC Institute of Metabolic Science, Addenbrooke's Hospital, University of Cambridge. Cambridge, UK.

[2]IMIBIC, Reina Sofia University Hospital, Cordoba, Spain.

[3]VTT Technical Research Centre of Finland, Espoo, Finland.

[4]Lipids and Atherosclerosis Research Unit, IMIBIC/Reina Sofia University Hospital, Spain.

[5]Department of Biochemistry (U38-FCT), Faculty of Medicine, University of Porto, Portugal.

[6]Departament de Bioquímica i Biologia Molecular, Universitat de Barcelona, 08028 Spain.

[7]Departamento de Farmacología, Universidad Complutense de Madrid, Spain.

[8]CIBER in Physiopathology of Obesity and Nutrition (CB06/03), Instituto de Salud Carlos III, Spain and Hospital Virgen de la Victoria, Malaga, Spain (IBIMA).

[9]College of Health, University of Utah, Salt Lake City, Utah.
[10]Division of Endocrinology, Metabolism, and Diabetes, University of Utah, Salt Lake City, Utah.
[11]Program in Cardiovascular and Metabolic Disorders, Duke-National University of Singapore Graduate Medical School, Singapore 169857

[12]Institute for Molecular Medicine Finland, Helsinki, Finland.

[13]Currently in Departamento de Bioquímica, Fisiología y Genética Molecular, Universidad Rey Juan Carlos, Spain.

[14]Wellcome Trust Sanger Institute, Hinxton, UK

Corresponding authors e-mail:

nuria.barbarroja.exts@juntadeandalucia.es;sr441@medschl.cam.ac.uk;ajv22@medschl.cam.ac.uk

Address reprint request to: Professor Antonio Vidal-Puig, Level 4, Institute of Metabolic Science, Box 289, Addenbrooke's Hospital, Cambridge, CB2 0QQ

Tel: 44-(0)1223762790 Fax: 44-(0)1223330598

RUNNING TITLE: *DEGS1*downregulation impairs adipocyte function.

Word count: 3997

Number of tables and figures: 7 figures and 1 table

ABSTRACT

Adipose tissue dysfunction is an important determinant of obesity-associated lipid induced metabolic complications. Ceramides are well known mediators of lipid induced insulin resistance in peripheral organs such as muscle. *DEGS1* is the desaturase catalysing the last step in the main ceramide biosynthetic pathway. Functional suppression of *DEGS1* activity results in substantial changes in ceramide species likely to affect fundamental biological functions such as oxidative stress, cell survival and proliferation. Here, we show that *degs1* expression is specifically decreased in the adipose tissue of obese patients and murine models of genetic and nutritional obesity. Moreover, loss of function experiments using pharmacological or genetic ablation of DEGS1 in preadipocytes prevented adipogenesis and decreased lipid accumulation. This was associated with elevated oxidative stress, cellular death and blockage of the cell cycle. These effects were coupled with increased dihydroceramide content. Finally, we validate *in vivo* that pharmacological inhibition of DEGS1 impairs adipocyte differentiation. These data identify *DEGS1* as a new potential target to restore adipose tissue function and prevent obesity-associated metabolic disturbances.

KEYWORDS: Adipocyte function, adipose tissue, *DEGS1*, obesity, insulin resistance and dihydroceramides

Dysfunction of white adipose tissue (WAT) and impaired differentiation of new adipocytes may lead to lipid leakage and inappropriate accumulation of ectopic lipids in peripheral organs, causing lipotoxicity and the Metabolic Syndrome(1). The toxic effects of lipids are determined by both the quantity and also by their qualitative characteristics(2). Whereas it is well documented that specific species of sphingolipids and ceramides mediate lipotoxicity in liver and muscle(3; 4), the contribution of specific lipotoxic species to WAT dysfunction in the context of obesity is still not well defined. It is known that in rodent WAT, ceramides increase in response to HFD(5; 6) concomitantly with the onset of insulin resistance(6). Lipid analysis of WAT from human obese subjects has produced conflicting results, showing either increased or decreased ceramide levels in obese and insulin resistant patients(7; 8).

Ceramides can be synthesised from sphingomyelins, but the main contributor to their biosynthesis is the *de novo* pathway. The final reaction of the *de novo* pathway is catalyzed by a Δ4-dihydroceramide desaturase (*DEGS1*) that adds a 4,5-trans-double bound on the sphingoid base of the dihydroceramide (DhCer) (9). The other enzyme, DEGS2 catalyzes the synthesis of phytoceramides(10), whose expression is restricted to skin, intestine and kidney.

There is evidence that downregulation of *degs1* increases the DhCer/Cer ratio in different cellular models. Although DhCer was considered an inactive precursor of ceramides(11), recent studies have suggested their relevance as modulators of cell cycle, apoptosis, autophagy or oxidative stress(12; 13), processes that *a priori* are expected to compromise the development and function of adipose tissue.

Since *DEGS1* is the key enzyme regulating the DhCer/Cer ratio, understanding its regulation is important in determining the pathophysiological relevance of this pathway in adipose tissue. Of note, degs1 has recently been identified in a GWAS study as a

candidate gene associated with fat mass accumulation in mice(14) further suggesting that *DEGS1* may be relevant for the adaptive accretion of adipose tissue. Moreover, *DEGS1* could be considered an attractive therapeutic target for obesity-associated insulin resistance, since Fenretinide has been claimed to improve insulin sensitivity *by inhibiting DEGS1*(15), although other molecular targets cannot be ruled out.

Here we show that *DEGS1* expression is selectively perturbed in the WAT of murine models of nutritional and genetically induced obesity and in WAT of morbidly obese patients. *In vitro* analysis revealed that both pharmacological inhibition and genetic ablation of DEGS1 results in impaired adipocyte differentiation and lipid accumulation, effects mediated by increased dihydroceramide content. In vivo, pharmacological inhibition of DEGS1 also resulted in impaired adipocyte differentiation. Decreased levels of DEGS1 were associated with increased oxidative stress, accelerated cellular death and blockage of cell cycle. We also show data supporting that *DEGS1* expression is regulated by PPARγ.

RESEARCH DESIGN AND METHODS

Mice husbandry

Animals were housed at 22-24°C with 12h light/dark cycles. Food and water were available *ad libitum*. Lean wildtype, PPARγ2$^{-/-}$ and PPARγ2$^{-/-}$xob/ob mice (POKO) (16) were used for profiling purposes. Mice were placed on a normal chow diet (D12450B) or in HFD (D12451) from Research Diets.

For the pharmacological inhibition of DEGS1, 10 weeks-old male C57BL/6 WT mice were used. Mice were given a HFD for 5weeks before C8-CPPC (Matreya) administration. All protocols used were approved by the UK Home Office.

Intraperitoneal injection of cyclopropenylceramide.

Mice were distributed in 2 groups (n=8) and administered daily vehicle (2-hydroxypropyl betacyclodextrine) or C8-CPPC (2mg/kg/day) for 9d via intraperitoneal injection. Mice were culled at the end of the experiment and WAT| was removed for gene expression and microscopy analysis. No differences in food intake, lean mass and fat content were observed during the treatment.

Ex vivo experiments in isolated mature adipocytes

Adipocytes from gonadal WAT of 16weeks C57BL/6 mice were obtained by collagenase type II digestion at 37ºC. After digestion, adipocytes were placed in DMEM media with or without 1μM C8-CPPC every 5h for a total period of 20h.

Retroviral Short Hairpin RNA Constructs for *DEGS1*

A RNAi-Ready pSIREN-RetroQ vectors (BD Biosciences) were used to target *degs1* in 3T3L1-cells. Sequences targeting *degs1* were ligated into the pSIREN vector as described in manufacturer's instructions. Retroviruses were generated by transfecting BOSC cells (ATCC) with the pSIREN plasmids using FuGene6 (Roche). Supernatant with the viral content was used to transfect 3T3-L1 preadipocytes. 24h after retroviral infection, the cells were selected with puromycin (4μg/ml).

Culture, differentiation and treatment of 3T3-L1 preadipocytes

Cells were differentiated into adipocytes (day9) accordingly to the protocol described in (17) with or without rosiglitazone 0.1μM. Lipid accumulation was assessed by Oil red O solution(18).

Pharmacological inhibition of *DEGS1* activity in vitro.

Effects on differentiation. At day 0 of differentiation, 3T3-L1 cells were treated with C8-CPPC 1μM and/or Rosiglitazone 0.1μM for 96h.

*Effects on lipolysis.*On day 8 of differentiation, after 48h treatment with C8-CPPC 1μM the cells were exposed to Noradrenaline (NA) (10^{-8} M and 10^{-7} M) for 6h.

Effects on insulin signalling. On day 8 of differentiation, after 48h treatment with C8-CPPC 1μM the cells were exposed to insulin (10nM and 100nM) for 15min.

Effects on glut4, adiponectin. On day 8 of differentiation, after 48h treatment with C8-CPPC 0.5-1μM the cells were exposed to insulin.

Effects on AMPK. On day 8 of differentiation, after 48h treatment with C8-CPPC 0.5-1μM the cells were exposed to insulin (10nM and 100nM), rosiglitazone (1nM and 10nM) and metformin (100nM) for 24h.

Dihydroceramide treatment.

3T3-L1 preadipocytes were treated at day 0 of differentiation with the induction cocktail and C2DhCer at 50μM for 3d, and a second batch of cells were exposed at day 3 of differentiation and treated with C2DhCer at 50μM for 3d. All batches were taken until final differentiation at day 9.

Human samples

The cohort included 28 morbidly obese (MO) and 6 non-obese subjects with no alterations to lipid or glucose metabolism, as controls (Table I). Approval for the study was given by the ethics committee and all patients gave their informed consent. Visceral adipose tissue biopsies were obtained from MO patients undergoing bariatric surgery (Scopinaro procedure) or laparoscopic surgery (hiatus hernia repair or cholecystectomies) for the lean subjects.

Western blotting

Protein extracts were prepared using the Nuclear and Cytoplasmic Extraction Reagents Kit (Pierce) according to manufacturer's instructions. Immunoblots were incubated with the following antibodies: PPARγ, C/EBPβ, CyclinA, (Santa Cruz) CyclinB1, D1, D3 and E1,cdk4, AKT, Ser473-pAKT, p44/42 MAPK, phospho-p44/42 MAPK, Ser660-pHSL, Ser565-pHSL, total HSL, ATGL, caveolin-1, plin1, glut4, adiponectin, and AMPK (Cell Signalling), adfp/adrp and abhd5 and anti-β-Actin (Abcam).

RT-PCR

RNA was extracted using TRI Reagent (Sigma) and reverse-transcribed to cDNA. Real-Time PCR using SYBRgreen was performed according to manufacturer's instructions (ABI). Primer sequences were obtained from Primer Blast(19). Expression of genes was corrected by the geometrical average of *18s*, β*2m*, *β-act*, and *36b4* using Bestkeeper (20).

Apoptosis: combined Annexin-V/propidium iodide staining

Viability was assessed by using an Annexin-V/propidium iodide kit (Bender MedSystems), according to manufacturer's recommendations. Binding of fluorescein-conjugated Annexin-V and propidium iodide was measured by FACSCalibur(BD).

Cellular proliferation:

Cell viability was assessed using an XTT colorimetric assay (Roche) following the protocol supplied by the manufacturer. Cell proliferation was analyzed by quantification of the incorporation of bromodeoxyuridine (Roche).

Bodipy staining, Reactive Oxygen Stress (ROS) production and mitochondrial content.

Cells were incubated with Bodipy at 4ºC or alternatively with 20µM DCF-DA or 100nM Mitotracker (Invitrogen) at 37°C for 30 min and analysed on a FACSCalibur.

Cellular oxygen consumption

Cells were exposed to oligomycin (1µM), C8-CPPC (0.9µM) and Antimycin/Rotenone (1µM each); O2 consumption was measured using the XF24 analyzer (Seahorse Bioscience) for a period of 90min.

Whole-mount confocal microscopy

Gonadal adipose tissue was fixed in 4% paraformaldehyde. Samples were incubated at 4°C with mouse pref-1 or rabbit Ki67 primary antibodies. Nuclei and neutral lipids were stained with Hoechst 33342, and BODIPY 493/503 respectively. Sample examination was performed using a Zeiss 510 confocal laser scanning microscope (Carl Zeiss). Pref1, Ki67, Bodipy positive cells and total cells (up to 913 cells/field) were automatically counted by using Image J software in 3 independent fields in each tissue.

Light microscopy analysis

Samples for adipose tissue H&E staining were prepared as described elsewhere (16). Adipocyte sizes were measured using Cell P (Olympus soft Imaging Solutions GMBH). Between 1000-3000 adipocytes from each mouse were used to obtain the mean cell-area.

Luciferase reporter assay

HEK293 cells were transfected using Lipofectamine LTX (Invitrogen), following the manufacturer's instructions. 75ng of the reporter plasmid (3xPPRE TKLuc) and 37.5ng

of the eukaryotic expression vector (pSV-PPARγ) were cotransfected to each well. The plasmid pRL-CMV (5ng/well) was included as an internal control. 24h post transfection cells were treated as indicated (DMSO, Rosiglitazone 10μM, GW1929 10μM, C2 and C16 DhCers and Cer 100 μM). Luciferase assays were performed using the dual luciferase reporter assay system (Promega).

Lipidomics

Cells were mixed with 0.9% NaCl and sonicated for 5 min at 5 ºC, 40 kHz. Samples were spiked with internal standard (IS). The samples were extracted with chloroform:methanol (2:1). The lower phase was collected and mixed with the labeled standard mixture (three stable isotope-labeled reference compounds). Lipid extracts were analyzed on a Q-ToF Premier mass spectrometer (Waters) combined with an Acquity Ultra Performance Liquid chromatography(UPLC/MS). The data was processed using MZmine software. The lipids were quantified by normalizing with corresponding IS.

Statistical analysis

Student t-test (unpaired), ANOVA and Duncan test were used for the statistical analysis. Statistically significance was set at $p<0.05$ and $p<0.01$. Spearman correlation was calculated to estimate the linear correlations between variables $p<0.01$.

RESULTS

DEGS 1 is downregulated in WAT in obese murine models.

Tissue distribution analysis showed that *degs1* is present in most tissues and it is particularly highly expressed in adipose tissue, liver and muscle, whereas *degs2* mRNA is only detected in intestine (Fig. 1A). *Degs1* expression *in vivo* was positively

correlated with WAT mass in lean healthy mice (Fig. 1B). However, this correlation was disrupted in murine models of nutritional and genetically induced obesity (HFD and ob/ob), where *degs1* mRNA expression was decreased vs. controls (Fig.1C and 1F). Of note, the dysregulation of *degs1* in obesity was limited to WAT, as its expression in liver or skeletal muscle was not affected in either HFD fed mice (Fig.1D and 1E) or in ob/ob mice (Fig.1G and H). DEGS1 was preferentially expressed in matured adipocytes vs. stromal vascular fraction (svf) in lean and ob/ob mice (Fig.S1) and downregulated in ob/ob adipocytes vs lean adipocytes. Moreover, this downregulation of *degs1* in total WAT of HFD fed and ob/ob mice was also recapitulated in visceral AT of morbidly obese patients (Fig S2A).

To determine whether the decrease in *degs1* expression was part of a global adaptation of *de novo* ceramide synthesis pathway in obesity, the expression of other genes in this pathway were measured. Expression of the *sptlc*1 and *sptlc*2 subunits were not changed in human visceral AT, nor in ob/ob WAT, but *sptlc*2 expression was increased in HFD WAT (Fig S2B-C). Moreover, both HFD and ob/ob mouse WAT exhibited a reduction in a subset of ceramide synthases, suggests a possible defect in the synthesis of specific subset of ceramides.

We then confirmed that modulators of obesity associated inflammation may contribute to the downregulation of *degs1,* as treatment of 3T3-L1 adipocytes with TNFα (5 ng/ml and 10ng/ml) for 48h resulted in a dose dependent downregulation of *degs1* mRNA expression (38.8±3.6% and 45.7±7.3% reduction respectively).

We then investigated a link between DEGS1 and the adipogenic programme. It is known that obese and insulin resistant murine models and humans have reduced expression of *pparγ2* in WAT. Furthermore we observed that expression of *pparγ2* and *degs1* were directly correlated in 3T3-L1 after treatment with Rosiglitazone (Fig.S3A).

To validate this *in vivo*, we analyzed the regulation of *degs1* in adipose tissue, liver and skeletal muscle of *pparγ2*KO and the POKO mice(16). WAT of *pparγ2*KO and POKO mice expressed significantly lower *degs1*mRNA levels vs. wt (Fig.S3B). This association was restricted to WAT since the expression of *degs1* in other metabolic organs such as skeletal muscle or liver was not affected when *pparγ2* was absent (Fig.S3C and D).

***DEGS1* controls important cellular functions such as proliferation, survival and oxidative stress in 3T3-L1 adipocytes.**

A stable *degs1* knock-down 3T3-L1 cell line (65%) (Fig.2A) resulted in inhibition of cell growth after 24h (Fig.2B-C). *Degs1* knock-down also induced cell death (13.7%) and apoptosis (6.3%)(Fig.2E). These were associated with a decrease in cyclin-A and cdk2 in *degs1*KD proliferating cells (Fig.2F) as well as elevated Bax and caspase-3mRNA (Fig.2D). Elevated reactive oxygen species (ROS) production (Fig.2I) along with an upregulation of the expression of antioxidant genes was observed in *degs1*KD preadipocytes (Fig.2H). This was accompanied by impaired mitochondrial oxygen consumption (Fig.2G) without changes in the number of mitochondria (Fig.2J).

***DEGS1* is required for adipocyte differentiation.**

Expression of *degs1* is increased during normal differentiation of 3T3-L1 adipocytes (Fig.3A). To investigate whether ablation of *DEGS1* affected adipogenesis, 3T3-L1 *degs1*KD cells were induced to differentiate. At d9, *degs1KD cells* showed impaired lipid accumulation vs. controls (Fig.3B). Moreover, *pref1* mRNA expression, a marker for preadipocytes was not decreased in *degs1*KD cells at d9 suggesting that a relevant number of cells remained in the preadipocyte stage (Fig.3C). In addition, expression of

proadipogenic and lipogenic genes were downregulated (Fig.3D). Interestingly, treatment with rosiglitazone only partially improved the differentiation and lipid accumulation rates of *degs1*KD cells (Fig. S4A-B).

We tested whether *DEGS1* expression may affect the mitotic clonal expansion (MCE). In *degs1*KD cells, *pparγ* and *cebpβ* were downregulated compared to controls at time 0 and 24h following differentiation induction (Fig. S5AB). The expression of *PPARγ* and several cyclins involved in adipogenesis were measured at earlier time points. We noted a strong effect of *degs1* depletion on PPARγ2 mRNA from time 0. Additionally, reduced levels of *degs1* blocked MCE as indicated by the inhibition of cyclin D1 and cdk2 expression between time 0 and 4h hours after the induction (Fig. S5AB). Cyclin E and cyclin D3 expression was also inhibited but at later time points.

Pharmacological inhibition of *DEGS1* recapitulates *DEGS1KD* antiadipogenic phenotype.

Use of C8-cyclopropenylceramide (C8-CPPC), a selective inhibitor of *DEGS1*(21) further confirmed the relevance of DEGS1 in adipogenesis. Similarly to degs1KD cells, 3T3-L1 cells were induced to differentiate and treated simultaneously with C8-CPPC from time 0h every 6h for 48h. C8-CPPC decreased the expression of proadipogenic transcription factors such as PPARγ and C/EBPβ as well as lipogenic genes (Fig. 4AC). The antiadipogenic effect of C8-CPPC persisted after Rosiglitazone treatment (Fig. 4AC). As expected, analysis of neutral lipids showed that 3T3-L1 cells treated with C8-CPPC for 96h accumulated significantly less lipids compared to untreated cells (Fig. 4D).

Pharmacological inhibition of DEGS1 also impairs adipocyte differentiation *in vivo.* We administered C8-CPPC IP to mice fed a HFD for 5weeks, an experimental protocol known to trigger adipocyte hyperplasia. Molecular analysis of the WAT from mice treated with C8-CPPC presented higher levels of pref-1+ cells, suggesting an increase in the number of preadipocytes vs. controls. Interestingly, a significant number of preadipocytes showed evidence of increased proliferation (Ki67+) whereas the number of differentiating preadipocytes (pref1+, bodipy +) was significantly smaller in comparison to controls (Fig.5A). These data were reinforced at mRNA level by showing increased expression of pref-1 and gata2 (Fig 5B) and the presence of less smaller adipocytes in treated mice (Fig.S6). Altogether, these data suggest C8-CPPC mediated inhibition of DEGS1 impaired the capacity of preadipocytes to differentiate into adipocytes *in vivo*.

DEGS1 is required for lipid accumulation, basal lipolysis and glucose uptake in mature adipocytes.

We next focused on the effects of DEGS1 inhibition in fully differentiated adipocytes by treating isolated mature adipocytes-from the gonadal adipose tissue of C57BL/6 mice- with C8-CPPC for 24h. C8-CPPC caused a decrease in the expression of lipid metabolism genes as well as an increase in antioxidant genes (Fig S7) recapitulating our observations in 3T3L1 preadipocytes.

We further investigated the effects of inhibiting DEGS1 on lipolytic activity and insulin signalling, and measured adiponectin expression as a representative fingerprint of global adipocyte homeostasis in mature differentiated 3T3L1 adipocytes. Thus, we observed that basal lipolytic activity was decreased in mature differentiated 3T3L1 adipocytes

when treated with C8-CPPC in non-stimulated conditions (Fig. 6A). Systematic evaluation of the lipolytic axis showed that under basal conditions, phosphorylation of Ser565 was also substantially increased by C8-CPPC concomitantly with a minor downregulation of Ser660 phosphorylation (Fig.6B-D) suggesting a decreased HSL activity. Moreover, total levels of HSL were also decreased in C8-CPPC treated cells. These data suggest that pharmacological inhibition of DEGS1 in mature adipocytes disrupts the lipolytic response under non-stimulated conditions a defect that was superseded in the presence of NA.

Finally we characterised the effects of pharmacological inhibition of DEGS1 on insulin signalling in 3T3-L1 mature adipocytes treated with C8-CPPC for 48h as described above, and subsequently incubated in the presence of increasing doses of insulin. No major differences where observed in the phosphorylation of AKT in C8-CPPC treated cells after acute insulin stimulation (Fig.6E). However, we found that Glut4 protein levels were increased in C8-CPPC treated cells, suggesting that glucose uptake may be increased (Fig.6F). Interestingly, we also did not observe any differences in either adiponectin levels in response to C8-CPPC or in AMPK phosphorylation, a known inducer of adiponectin, although increased levels of tAMPK were observed (Fig 6GH).

Both, Pharmacological and Genetic inhibition of *DEGS1* increases dihydroceramide/ceramide ratio in 3T3-L1-cells.

We confirmed that C8-CPPC increased the DhCer/Cer ratio in 3T3L-1 preadipocytes upon inhibition of *DEGS1* (Fig.4E). Similarly, *degs1*KD preadipocytes (d0) exhibited an increased DhCer/Cer ratio vs. controls. Downregulation of *degs1* expression in *degs1*KD cells was accompanied by a dowregulation of serine palmitoyltransferase

(*sptlc*1) and Ceramide synthase 6 (*Cers*6), suggestive of a homeostatic readjustment of the biosynthetic pathway to compensate for the dysfunction of degs1. Other genes related to ceramide homeostasis such as neutral ceramidase (*ncdase*), and glycosylceramide synthase (*gcs*) were also downregulated.

Curiously, at d9, *degs1*KD cells, despite impaired differentiation, showed a complete restoration of the DhCer/Cer ratio (indicated by the normalization of the ceramide pool) (Fig.S8A). This could be partially explained by a compensation mechanism, mediated by downregulation of neutral ceramidases and the conversion of sphyngomyelins to ceramides (upregulation of sphyngomyelinase 2) (Fig.S8B).

The Impairment of adipocyte differentiation during early adipogenesis by DEGS1 inhibition is recapitulated by Dihydroceramides per se.

We finally sought to validate whether DhCer by itself could mediate the effects of DEGS1 inhibition on adipocyte differentiation in our models of genetic or pharmacological inhibition of degs1. 3T3-L1cells were treated with C2-DhCer during a) the MCE at time 0 and b) at day 3 after differentiation. DhCer inhibited lipid accumulation (Fig.7A) and the expression of genes involved during the early stages of adipogenesis (Fig. 7B).

Since synthetic sphingolipid analogues are known to modulate PPARs activity(22), we investigated whether both C2 and C16 DhCer could exert a repressive effect on PPARγ activation in the presence of the PPARγ ligands (Fig. 7C). Our results show that DhCer can also block the ligand-mediated transactivation of PPARγ. Similar results were obtained with ceramides, indicating these effects were not a consequence of the unsaturation of the sphingoid moiety (data not shown).

DISCUSSION

The DhCer/Cer ratio has an important homeostatic regulatory role in the cell, contributing to cell survival, autophagy and oxidative stress(12; 13). Here we identify DEGS1 as an essential metabolic enzyme which is dysregulated in obese states and contributes to adipose tissue dysfunction. Our complementary *in vitro* and *in vivo* approaches reveal that reduced DEGS1 function impairs adipogenesis and lipogenesis programmes and increases oxidative stress.

DEGS1 is expressed in WAT and correlates in rodents with fat mass in healthy states, an association that is disrupted in severe forms of obesity. Expression of *DEGS1* in liver or muscle is not affected by obesity, further indicating that the WAT is particularly susceptible to changes in ceramide metabolism in obese states. The relevance to human obesity is confirmed by the downregulation of *DEGS1* in the adipose tissue of morbidly obese patients, and by recent reports showing that DhCer rather than Cer content positively correlates with BMI and waist circumference in cohorts of overweight-obese subjects(23; 24). To date, only a single functional mutation in the *Degs1*gene has been reported in humans where patients demonstrate increased serum DhCer and decreased cholesterol esters, and decreased waist to hip ratio(25). Globally considered, these data suggest the existence of an association between *DEGS1* function and fat mass.

The molecular mechanism leading to the defective adipose tissue expression of *degs1* in human and rodent obesity is unknown. Here, we have shown that TNFα, a mediator of obesity induced inflammation and insulin resistance, decreases the transcriptional expression of *degs1* in cultured adipocytes, which suggests that low chronic inflammation may contribute to *DEGS1* dysfunction. Other obesity associated processes, such as increased oxidative stress and hypoxia, have been shown to impair *DEGS1* activity and increase DhCer levels(26). Our results also show a positive association between levels of the proadipogenic *pparγ2* isoform and *degs1* in adipose

tissue, and given the documented downregulation of *pparγ2* in adipose tissue in obese insulin resistant states, it is conceivable that decreased levels of *pparγ2* may contribute to the defective expression of *degs1* associated to obesity.

Studies in rodents have shown that Cer are increased in the WAT of animals fed HFD(5) concomitantly with the onset of insulin resistance(6). Results from ob/ob mice and human obese studies are more unclear, where both increased or decreased levels of ceramides have been reported(7; 8). This suggests that Cer synthesis may be dependent on the severity of the obese state and the strength of the adaptive homeostatic responses attempting to restore their normal balance.

Our pharmacological and gene ablation studies have shown that inhibition of *DEGS1* is associated with oxidative stress, cellular death, impaired adipocyte differentiation, impaired lipid accumulation and impaired basal lipolysis in mature adipocytes.

Our *in vitro* studies revealed that the defect in adipogenesis programme caused by depletion of *DEGS1* occurs during the early stages of adipogenesis (MCE) when PPARγ controls the expression of genes that regulate the cell cycle, by directly interacting with cyclin D3. Another cyclin involved in adipocyte differentiation is cyclin D1, and here we show that downregulation of *DEGS1* blocks PPARγ activity and cyclins such as D1, D3, E, as well as decreasing cdk2, which modulates PPARγ activity during adipogenesis. These data are consistent with studies showing that downregulation of *degs1* by siRNA inhibits cell growth and arrests the cell cycle in cancer cells(12), and where its overexpression increased cell migration and metastasis(27).

The pharmacological inhibition of DEGS1 in vivo validated the results obtained in vitro and strengthen the concept that functional *degs1* is required for the full differentiation of preadipocytes into mature adipocytes.

We also provide evidence that both pharmacological and genetic ablation of *degs1* certainly increased DhCer levels in in vitro models which according to our results in in vitro models may directly block adipocyte differentiation and lipid deposition. This effect on lipid accumulation was more severe when the treatment was administered during the first three days of differentiation, suggesting a direct impact of DhCer accumulation during early stages of adipogenesis. We also provide evidence showing that accumulation of DhCers can also directly repress the transcriptional activity of PPARγ and hence could contribute to impair the capacity of the preadipocytes to develop a full adipogenic programme.

These observations strengthen the concept that DhCers are not merely inert precursors of ceramides. Nevertheless, the molecular mechanism linking DhCers accumulation and dysregulation of the cell cycle and other cellular events remains elusive. One possible mechanism is that changes in the DhCer/Cer ratio may disrupt membrane dependent structures by altering the levels of cholesterol and/or caveolin in lipid rafts, which are known to be highly sensitive to sphingomyelin pool. Alternatively, changes in the DhCer/Cer ratio may disturb the global phospholipidome, potentially altering membrane-associated processes relevant to adipocyte function. These are important questions to address in future research.

In summary, our results indicate that defects in DEGS1 in the context of the MetS may compromise adipose tissue expansion and function through the combined inhibition of adipogenesis, promotion of cell death and oxidative stress due to the direct accumulation of DhCers. Thus, our data suggests that the selective manipulation of *DEGS1* and/or its substrates in WAT may be a pathophysiologically advantageous

strategy to improve adipose tissue homeostasis and ameliorate the burden of obesity associated metabolic complications.

ACKNOWLEDGMENTS

We thank Dr. Carobbio Mrs. Peirce and Ms. Philips (Wellcome Trust-MRC IMS, University of Cambridge, UK) for their excellent technical advice, support and suggestions. This work was funded by Medical Research Council, MDU MRC, FP7-ETHERPATHS and the British Heart Foundation (BHF). We declare no conflict of interest.

NB and SRC, AC, JRP, AP, ICB, VP, GMG and CLP performed the *in vitro and ex vivo* experiments, collected and analyzed the data. HN and MO developed analytical platforms and performed and analysed lipidomic experiments. NB, FJT held and characterized the human cohorts, collected gene expression data from adipose depots, and analyzed the data. NB, SRC, AJS, SS and AVP designed the experiments. NB, SRC, HN, AC, JRP, AP, ICB, VP, GMG, CLP, FJT, AJS, SS, MO and AVP discussed the manuscript. NB, SRC and AVP coordinated and directed the project. NB, SRC and AVP developed the hypothesis and wrote the manuscript.

REFERENCES

1. Montague CT, O'Rahilly S: The perils of portliness: causes and consequences of visceral adiposity. Diabetes 2000;49:883-888
2. Carobbio S, Rodriguez-Cuenca S, Vidal-Puig A: Origins of metabolic complications in obesity: ectopic fat accumulation. The importance of the qualitative aspect of lipotoxicity. Curr Opin Clin Nutr Metab Care 2011;14:520-526
3. Chavez JA, Summers SA: Lipid oversupply, selective insulin resistance, and lipotoxicity: molecular mechanisms. Biochim Biophys Acta 2010;1801:252-265
4. Chavez JA, Summers SA: A ceramide-centric view of insulin resistance. Cell Metab 2012;15:585-594
5. Shah C, Yang G, Lee I, Bielawski J, Hannun YA, Samad F: Protection from high fat diet-induced increase in ceramide in mice lacking plasminogen activator inhibitor 1. J Biol Chem 2008;283:13538-13548
6. Turner N, Kowalski GM, Leslie SJ, Risis S, Yang C, Lee-Young RS, Babb JR, Meikle PJ, Lancaster GI, Henstridge DC, White PJ, Kraegen EW, Marette A, Cooney GJ, Febbraio MA, Bruce CR: Distinct patterns of tissue-specific lipid accumulation during the induction of insulin resistance in mice by high-fat feeding. Diabetologia 2013;56:1638-1648
7. Blachnio-Zabielska AU, Koutsari C, Tchkonia T, Jensen MD: Sphingolipid content of human adipose tissue: relationship to adiponectin and insulin resistance. Obesity (Silver Spring) 2012;20:2341-2347
8. Blachnio-Zabielska AU, Pulka M, Baranowski M, Nikolajuk A, Zabielski P, Gorska M, Gorski J: Ceramide metabolism is affected by obesity and diabetes in human adipose tissue. J Cell Physiol 2012;227:550-557
9. Ternes P, Franke S, Zahringer U, Sperling P, Heinz E: Identification and characterization of a sphingolipid delta 4-desaturase family. J Biol Chem 2002;277:25512-25518
10. Mizutani Y, Kihara A, Igarashi Y: Identification of the human sphingolipid C4-hydroxylase, hDES2, and its up-regulation during keratinocyte differentiation. FEBS Lett 2004;563:93-97
11. Ahn EH, Schroeder JJ: Induction of apoptosis by sphingosine, sphinganine, and C(2)-ceramide in human colon cancer cells, but not by C(2)-dihydroceramide. Anticancer Res 2010;30:2881-2884
12. Kraveka JM, Li L, Szulc ZM, Bielawski J, Ogretmen B, Hannun YA, Obeid LM, Bielawska A: Involvement of dihydroceramide desaturase in cell cycle progression in human neuroblastoma cells. J Biol Chem 2007;282:16718-16728
13. Siddique MM, Li Y, Wang L, Ching J, Mal M, Ilkayeva O, Wu YJ, Bay BH, Summers SA: Ablation of dihydroceramide desaturase 1, a therapeutic target for the treatment of metabolic diseases, simultaneously stimulates anabolic and catabolic signaling. Mol Cell Biol 2013;33:2353-2369
14. Parks BW, Nam E, Org E, Kostem E, Norheim F, Hui ST, Pan C, Civelek M, Rau CD, Bennett BJ, Mehrabian M, Ursell LK, He A, Castellani LW, Zinker B, Kirby M, Drake TA, Drevon CA, Knight R, Gargalovic P, Kirchgessner T, Eskin E, Lusis AJ: Genetic control of obesity and gut microbiota composition in response to high-fat, high-sucrose diet in mice. Cell Metab 2013;17:141-152
15. Bikman BT, Guan Y, Shui G, Siddique MM, Holland WL, Kim JY, Fabrias G, Wenk MR, Summers SA: Fenretinide prevents lipid-induced insulin resistance by blocking ceramide biosynthesis. J Biol Chem 2012;287:17426-17437
16. Medina-Gomez G, Gray SL, Yetukuri L, Shimomura K, Virtue S, Campbell M, Curtis RK, Jimenez-Linan M, Blount M, Yeo GS, Lopez M, Seppanen-Laakso T,

Ashcroft FM, Oresic M, Vidal-Puig A: PPAR gamma 2 prevents lipotoxicity by controlling adipose tissue expandability and peripheral lipid metabolism. PLoS Genet 2007;3:e64
17. Roberts LD, Virtue S, Vidal-Puig A, Nicholls AW, Griffin JL: Metabolic phenotyping of a model of adipocyte differentiation. Physiol Genomics 2009;39:109-119
18. Ramirez-Zacarias JL, Castro-Munozledo F, Kuri-Harcuch W: Quantitation of adipose conversion and triglycerides by staining intracytoplasmic lipids with Oil red O. Histochemistry 1992;97:493-497
19. Ye J, Coulouris G, Zaretskaya I, Cutcutache I, Rozen S, Madden TL: Primer-BLAST: a tool to design target-specific primers for polymerase chain reaction. BMC Bioinformatics 2012;13:134
20. Pfaffl MW, Tichopad A, Prgomet C, Neuvians TP: Determination of stable housekeeping genes, differentially regulated target genes and sample integrity: BestKeeper--Excel-based tool using pair-wise correlations. Biotechnol Lett 2004;26:509-515
21. Triola G, Fabrias G, Llebaria A: Synthesis of a Cyclopropene Analogue of Ceramide, a Potent Inhibitor of Dihydroceramide Desaturase. Angew Chem Int Ed Engl 2001;40:1960-1962
22. Tsuji K, Satoh S, Mitsutake S, Murakami I, Park JJ, Li Q, Chang YT, Chung SK, Igarashi Y: Evaluation of synthetic sphingolipid analogs as ligands for peroxisome proliferator-activated receptors. Bioorg Med Chem Lett 2009;19:1643-1646
23. Mamtani M, Meikle PJ, Kulkarni H, Weir JM, Barlow CK, Jowett JB, Bellis C, Dyer TD, Almasy L, Mahaney MC, Duggirala R, Comuzzie AG, Blangero J, Curran JE: Plasma dihydroceramide species associate with waist circumference in Mexican American families. Obesity (Silver Spring) 2014 Mar;22(3):950-6.
24. Weir JM, Wong G, Barlow CK, Greeve MA, Kowalczyk A, Almasy L, Comuzzie AG, Mahaney MC, Jowett JB, Shaw J, Curran JE, Blangero J, Meikle PJ: Plasma lipid profiling in a large population-based cohort. J Lipid Res 2013;54:2898-2908
25. Curran J, Meikle P, Weir J, Jowett J. Deep Sequencing in Extended Pedigrees Reveals a Major Rare Non-Synonymous Variant Influencing the De Novo Ceramide Synthesis Pathway. Abstract presented in *American Society of Human Genetics meeting*. Boston, 2013.
26. Idkowiak-Baldys J, Takemoto JY, Grilley MM: Structure-function studies of yeast C-4 sphingolipid long chain base hydroxylase. Biochim Biophys Acta 2003;1618:17-24
27. Zhou W, Ye XL, Sun ZJ, Ji XD, Chen HX, Xie D: Overexpression of degenerative spermatocyte homolog 1 up-regulates the expression of cyclin D1 and enhances metastatic efficiency in esophageal carcinoma Eca109 cells. Mol Carcinog 2009;48:886-894

FIGURE LEGENDS

FIG.1.(A)Tissue distribution of degs1 (B) Correlation of degs1 mRNA expression and fat pad size. The Spearman correlation coefficients were calculated to estimate the linear correlations between variables. The rejection level for a null hypothesis was $p < 0.01$. Data from 14 lean mice (C-E) Expression levels of *degs1* mRNA in response to HFD (F-H)Expression levels of *degs1* mRNA in ob/ob mice. Mean ± Sem for 6 to 8 animals per group. *$p<0.05$ vs. wt. WAT, white adipose tissue; BAT, brown adipose tissue; SKM, skeletal muscle: HFD, High fat diet; WT, wild type; IngFat; Inguinal Fat; gWAT; gonadal white adipose tissue.

FIG.2(A)mRNA expression of *degs1* in 3T3-L1 treated with shRNA against *degs1*(B and C)Cell proliferation (XTT and BrdU assays every 24h until 96h and 72h respectively)(D) mRNA expression of *Cdk2, Bcl2, Bax* and *Caspase3*. (E) Apoptosis and cell death rate (F) Protein expression of Cdk2 (G) Oxygen consumption rate (OCR) (H)mRNA expression of antioxidant machinery genes. (I)Reactive oxidative species production (ROS)(J)Mitochondria levels. All these experiments were perfomed in degs1KD and wild type 3T3-L1 cells. Mean±Sem of three separate experiments performed in triplicate; *$p< 0.05$.

FIG.3.(A)mRNA expression of degs1 in 3T3-L1 cells during adipocyte differentiation.(B)Lipid accumulation at d9 of differentiation, Oil Red O Staining (C) mRNA expression of PREF1 in wild type and degs1 KD cells during differentiation. (D)mRNA expression of genes involved in adipocyte differentiation and lipid accumulation. Mean±Sem of three separate experiments performed in triplicate; *$p< 0.05$.

FIG.4. 3T3-L1 cells treated with C8-CPPC and/or Rosiglitazone (A and B) mRNA expression of genes involved in adipocyte differentiation and lipid accumulation at 24 and 48h after induction. (C) Protein expression levels of PPARγ2 and cEBPα (D) Lipid content after 48 and 96h of differentiation. Mean ± Sem of two separate experiments performed in triplicate. One way ANOVA was used to analyze statistical significance between treatments at 24 h and 48 h. Significant differences (Duncan; $p<0.05$) are indicated with different words. (E) Dihydroceramide and ceramide levels after 48h of differentiation. Mean ± Sem of two separate experiments performed in triplicate $p<0.05$.

FIG.5. C8-CCP inhibitor increases proliferation and decreases lipid accumulation in preadipocytes *in vivo***.** 10 weeks old mice were given a 45% HF diet for 5 weeks before treated intraperitoneally with vehicle or C8-CCP inhibitor (2mg/kg/day) during 9 days. (A) Representative images of immunofluorescence analysis of gonadal adipose tissue of control (vehicle) and C8-CCP-treated mice are presented with Pref-1 (*Cyan*) and ki-67 (*red, white arrows*). Nuclei and lipids are respectively stained with Hoechst (*blue*) and Bodipy (*green*). Scale bar 100 or 20 μm. Quantification of preadipocytes (left graph, % Pref-1 positive cells/total cells) and Ki67 (white bars) /Bodipy (dark grey bars) positive cells among preadipocytes (Pref-1 positive cells, grey bars). (B) mRNA expression of preadipocyte markers and pparg, desg1, adiponectin, caspase 3 and fas in gonadal adipose tissue of control and C8-CCP-treated mice. n=7-8 mice per experimental group; mean±SEM;*$p<0.05$, ***$p<0.0001$ versus vehicle

FIG.6. (A) Glycerol release in 3T3-L1 adipocytes exposed 48h with C8-CPPC and stimulated with nor-adrenalin (NA) for 6h. (B-D) Results from Western blot analysis for p-HSL/HSL ratio and total HSL in 3T3L1 adipocytes exposed 48h with C8-CPPC and stimulated with NA for 6h. Graphs show the mean ± SEM of two separated

experiments; $p< 0.05$, $^{\&}p<0.05$ vs cells without NA and $^{\#}p<0.05$ vs cells without NA or treated with 10^{-8}M NA. (E) Effects of pharmacological inhibition of DEGS1 on insulin signalling. Results from Western blot analysis for p-AKT and AKT in 3T3-L1 adipocytes exposed 48h or 72h with C8-CPPC 1μM and increased concentrations of Insulin (10 nM-100 nM) for 15min. (F and G9) Results from Western blot analysis for Glut4 and adiponectin in 3T3-L1 adipocytes exposed with C8-CPPC 0.5-1μM and Insulin (100 nM) for 48 hours. (H) Results from Western blot analysis for AMPK in 3T3-L1 adipocytes exposed with C8-CPPC 0.5-1μM and insulin (100nM), rosiglitazone (1 nM) and metformin (100 nM) for 48 hours. $^{b}p< 0.05$ versus untreated cells (Insulin, Rosi or Metformin effect) and; $^{b}p< 0.05$ versus 0 μM C8-CPPC (C8-CPPC effect)

FIG.7. (A and B) Dihydroceramides impair adipocyte differentiation during early adipogenesis. 3T3L1 preadipocytes treated withC2-DhC (50μM) for a period of 48h at d0 or at d3 of differentiation. ORO staining and mRNA expression of adipogenesis and lipid metabolism genes. Mean ± Sem of two separated experiments performed in triplicate; $*p< 0.05$ vs. control. (C) Dihydroceramides decrease ligand-mediated PPARγ transactivation. Cells were treated with DMSO as a control group, Rosiglitazone 10uM, GW1929 10uM, C2 and C16 dihydroceramides and ceramides 100 uM as indicated. Graphs represent the average of 3 independent experiments. $p< 0.05$. (*) vs control cells, (#) vs Rosiglitazone and (&) vs GW1929.

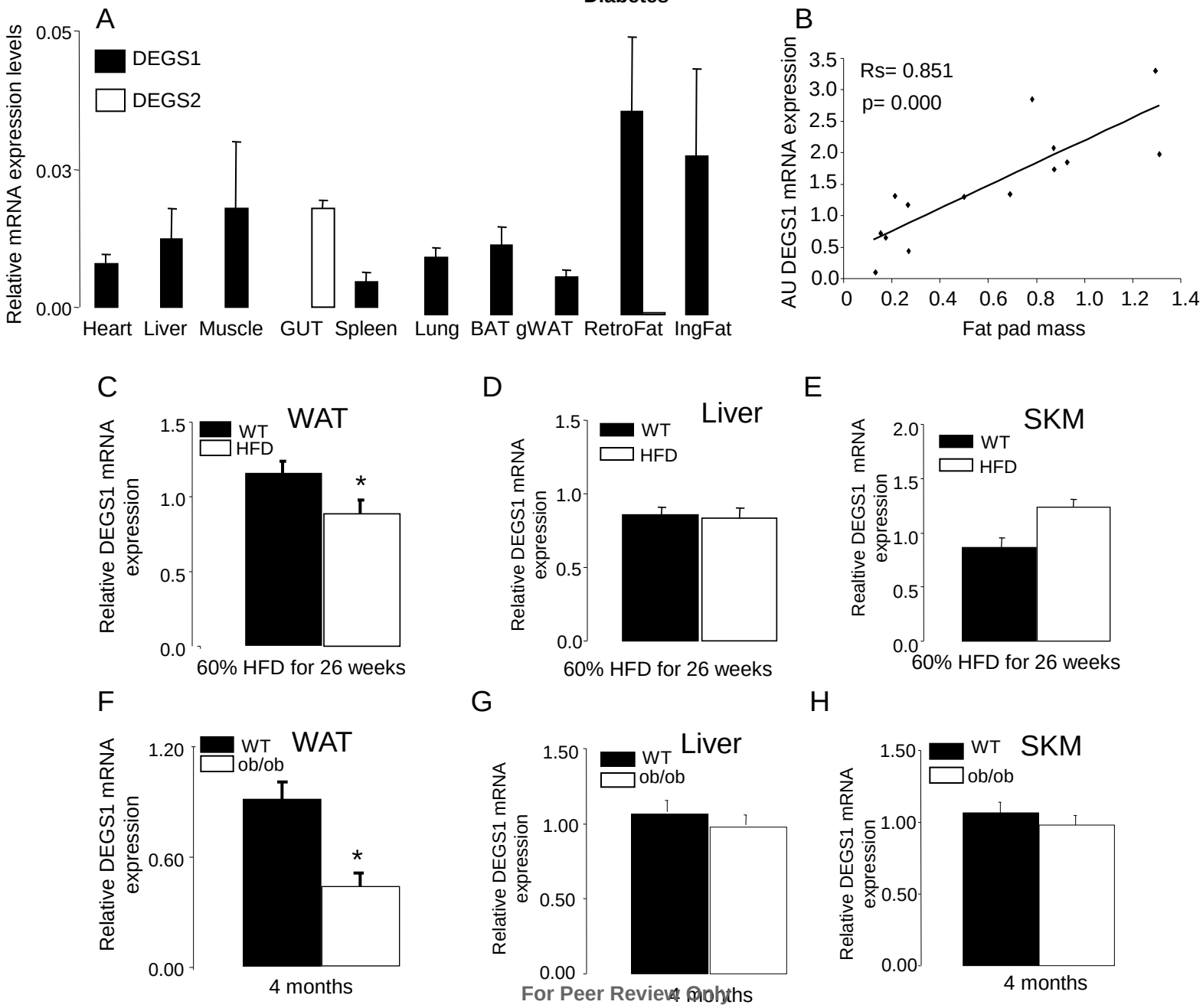

Figure 1

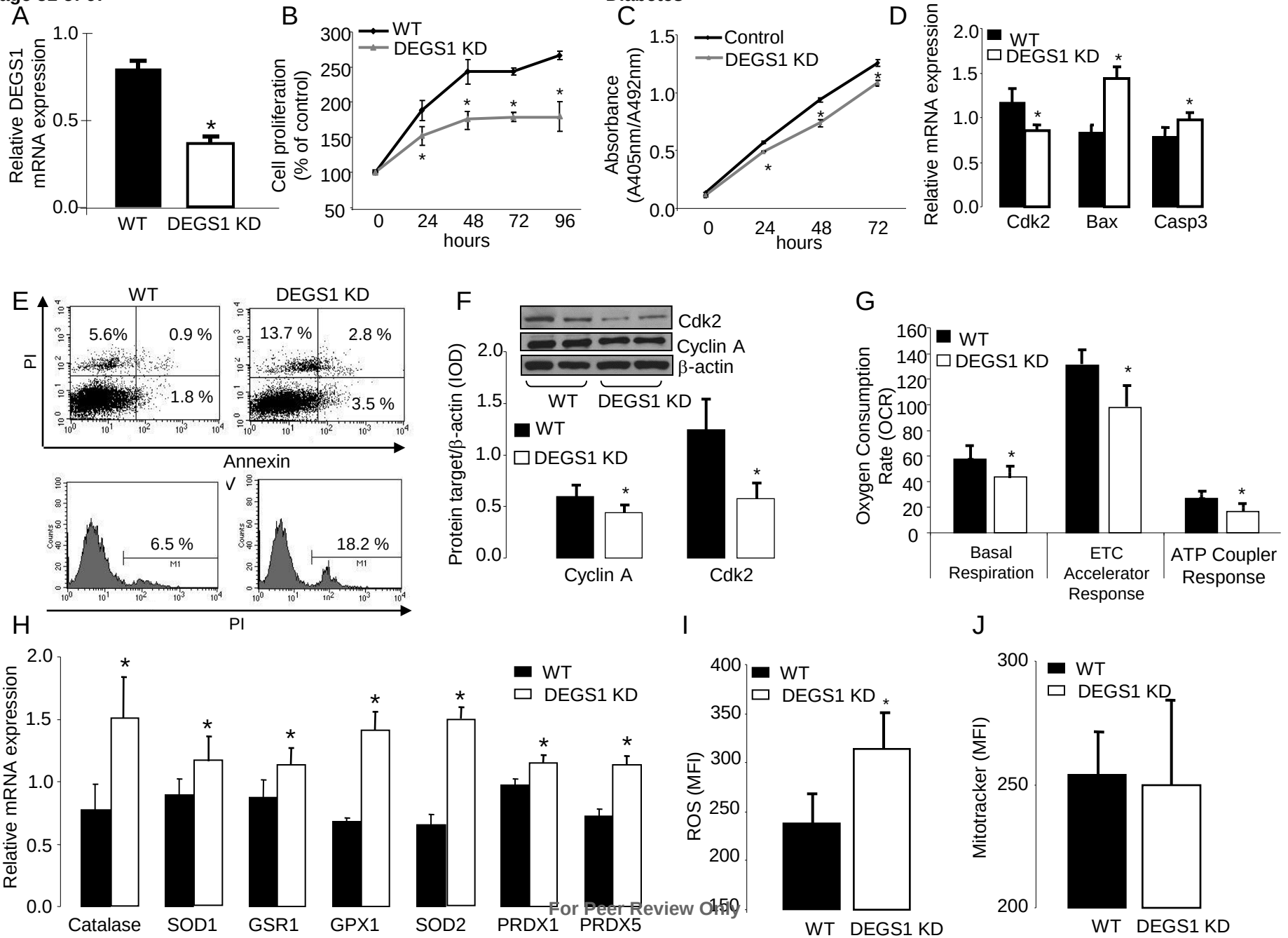

Figure 2

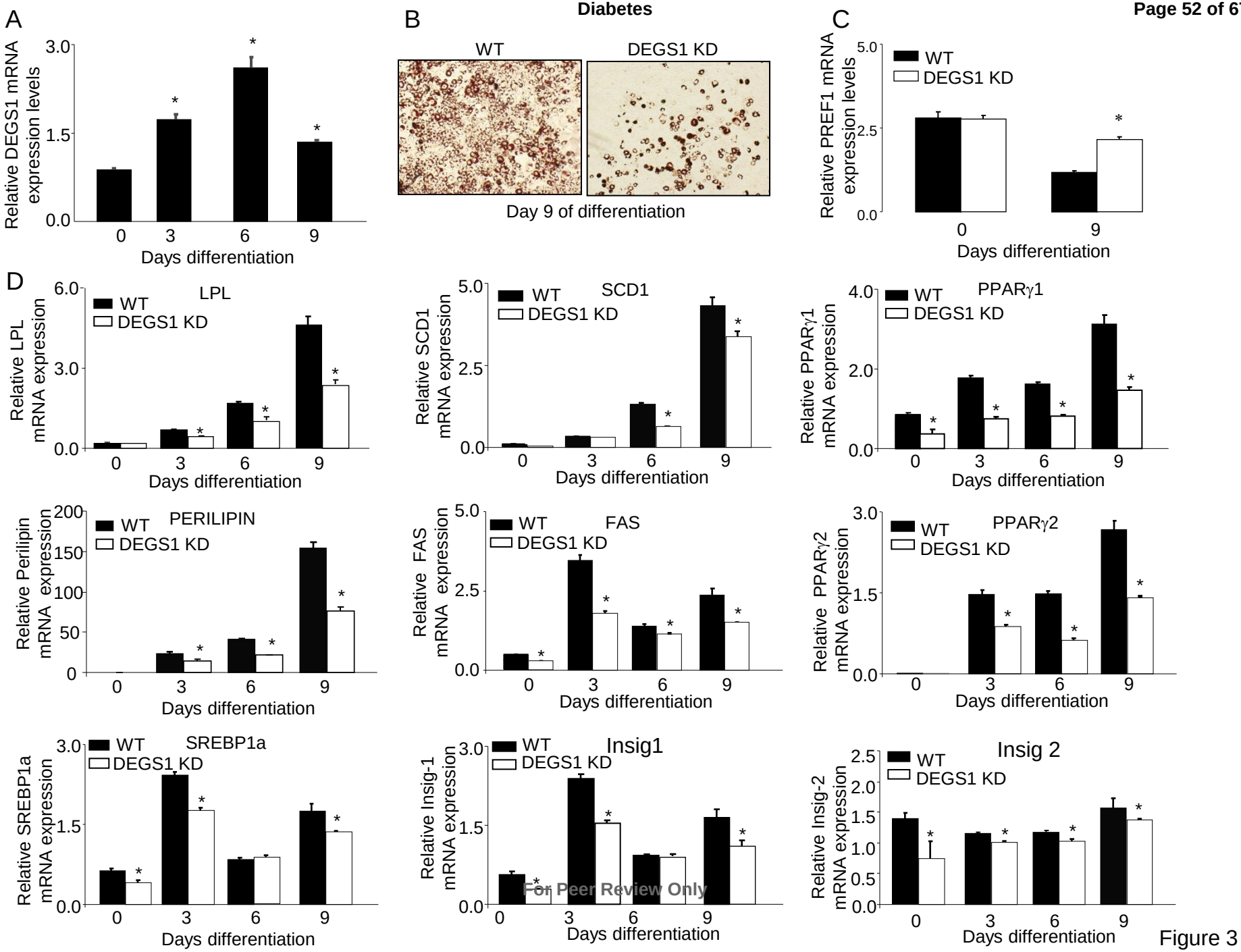

Figure 3

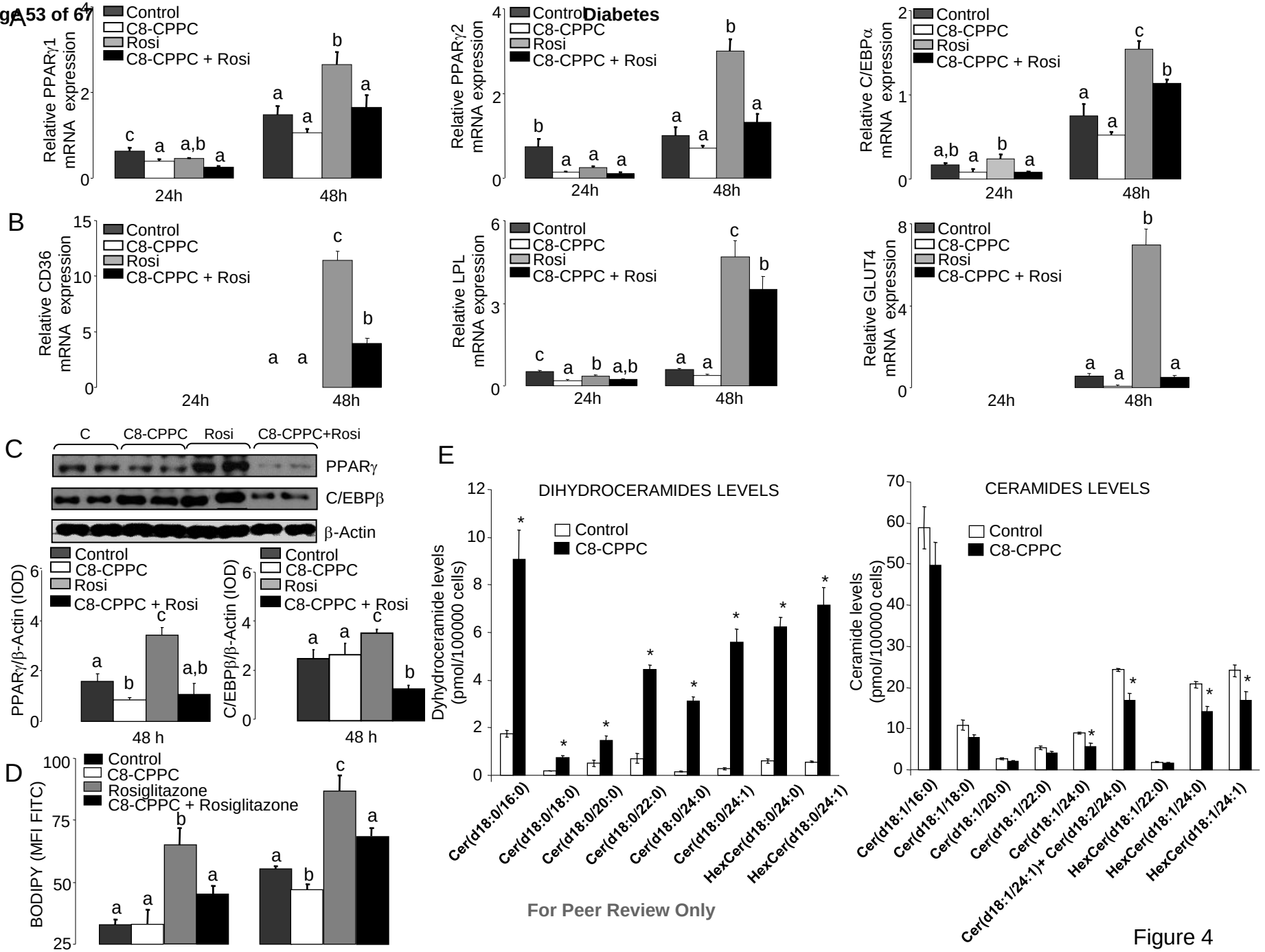

Figure 4

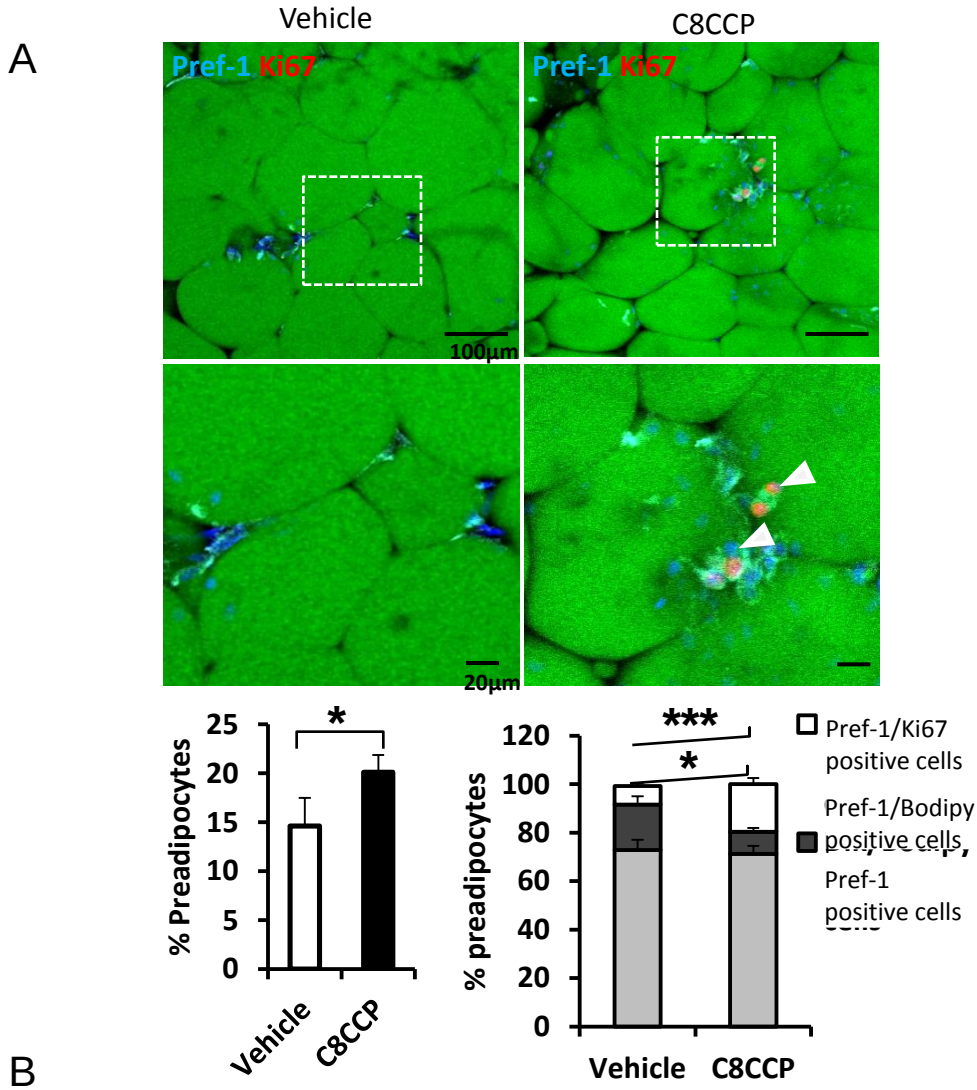
A
Vehicle
C8CCP
Pref-1 Ki67
Pref-1 Ki67
100µm
20µm
% Preadipocytes
25
20
15
10
5
0
*
Vehicle
C8CCP
% preadipocytes
120
100
80
60
40
20
0
***
*
Pref-1/Ki67 positive cells
Pref-1/Bodipy positive cells
Pref-1 positive cells
Vehicle
C8CCP

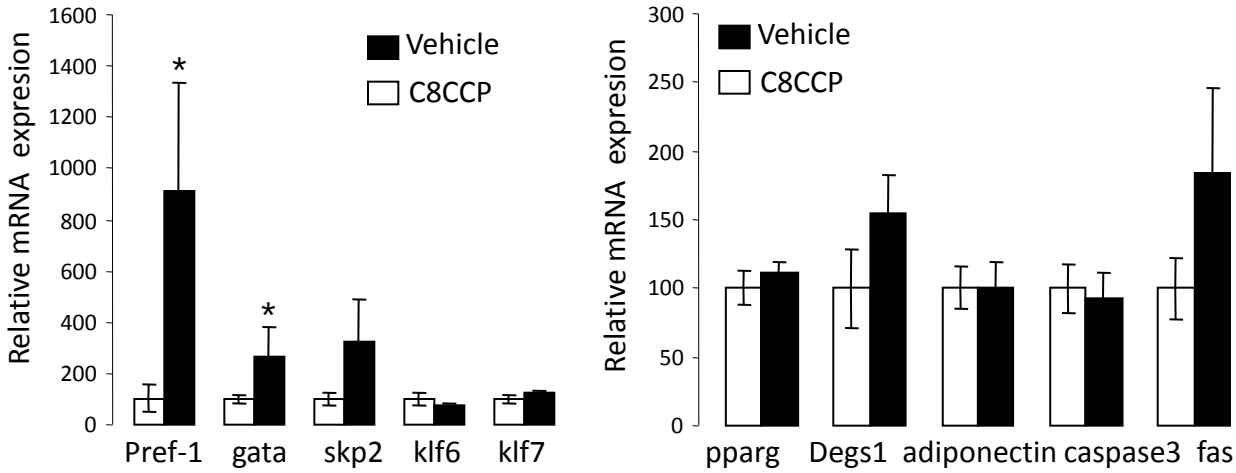
B
Relative mRNA expresion
1600
1400
1200
1000
800
600
400
200
0
*
*
Vehicle
C8CCP
Pref-1
gata
skp2
klf6
klf7
Relative mRNA expresion
300
250
200
150
100
50
0
Vehicle
C8CCP
pparg
Degs1
adiponectin
caspase3
fas

Figure 5

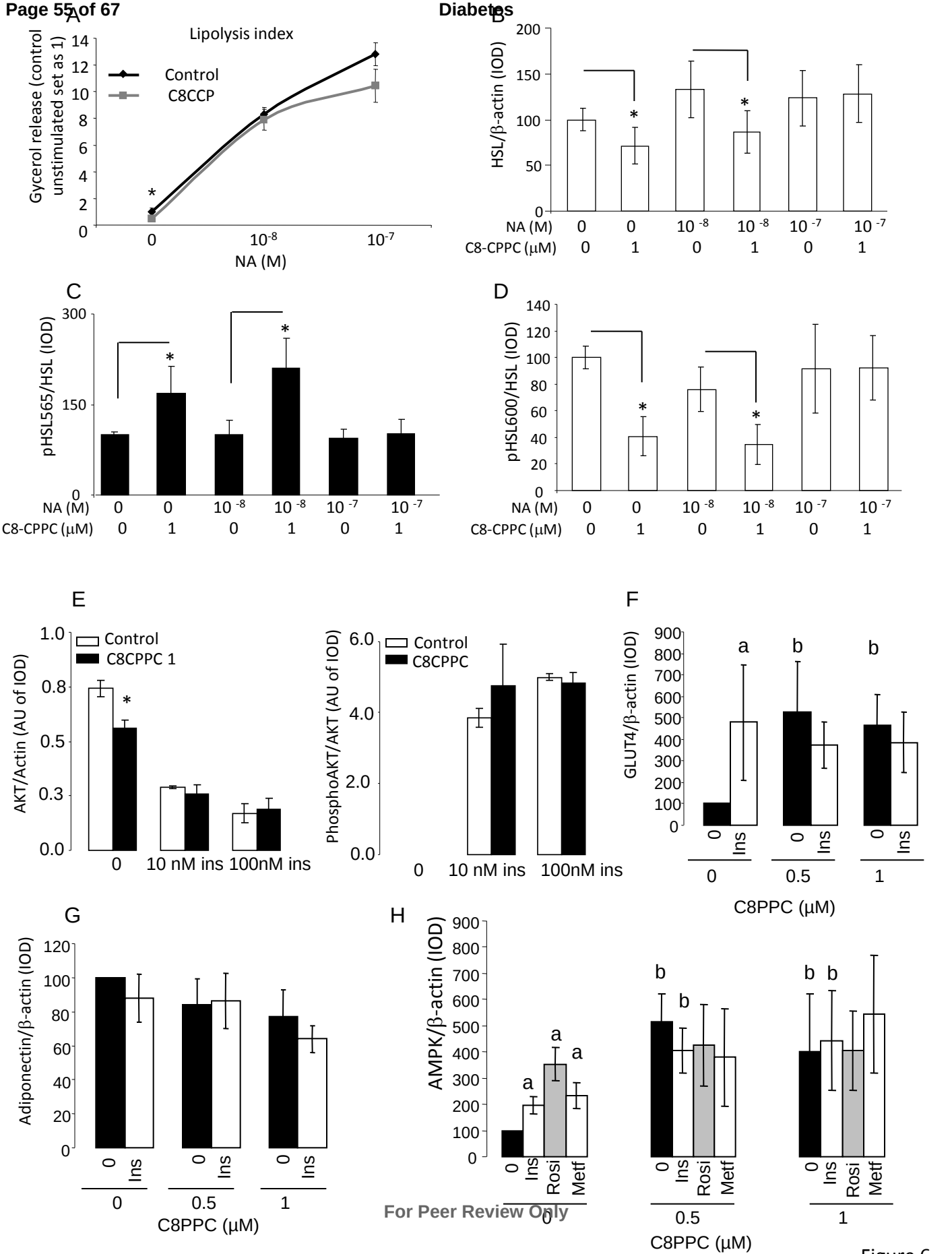

Figure 6

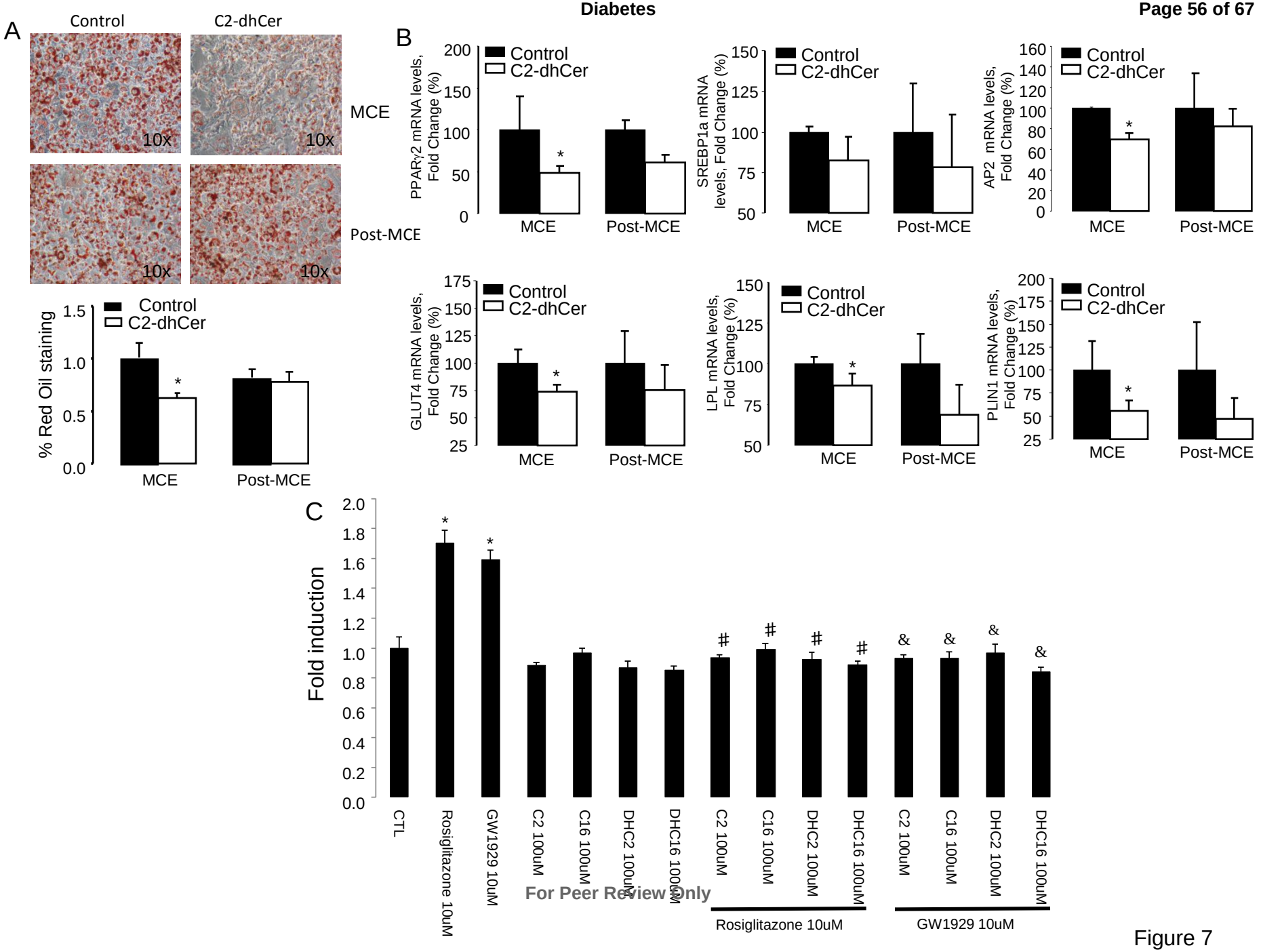

Figure 7

Table1. Clinical characteristics of controls and morbidly obese patients

	Controls	Morbidly obese
Male/Female	3/3	14/14
Age, years	52.17± 5.1	41.57 ± 2.96
Weight, Kg	74.00 ± 0.71	155.5 ± 7.32
Height, cm	162.60 ± 1.60	165.53 ± 2.49
BMI, Kg/m2	25.04 ± 0.55	56.51 ± 1.68
Serum insulin, UI/ml	11.23 ± 1.58	30.09 ± 2.30
HOMA-IR	3.51 ± 0.48	8.18 ± 0.78
Serum glucose, mmol/l	6.03 ± 0.32	5.74 ± 0.26
Serum cholesterol, mmol/l	4.68 ± 0.40	4.92 ± 0.25
HDL cholesterol, mmol/l	0.97 ± 0.23	1.10 ± 0.09
Triglycerides, mmol/l	1.08 ± 0.20	1.42 ± 0.19

[1] Values are means ± SEM. HDL-c= High density lipoprotein-cholesterol

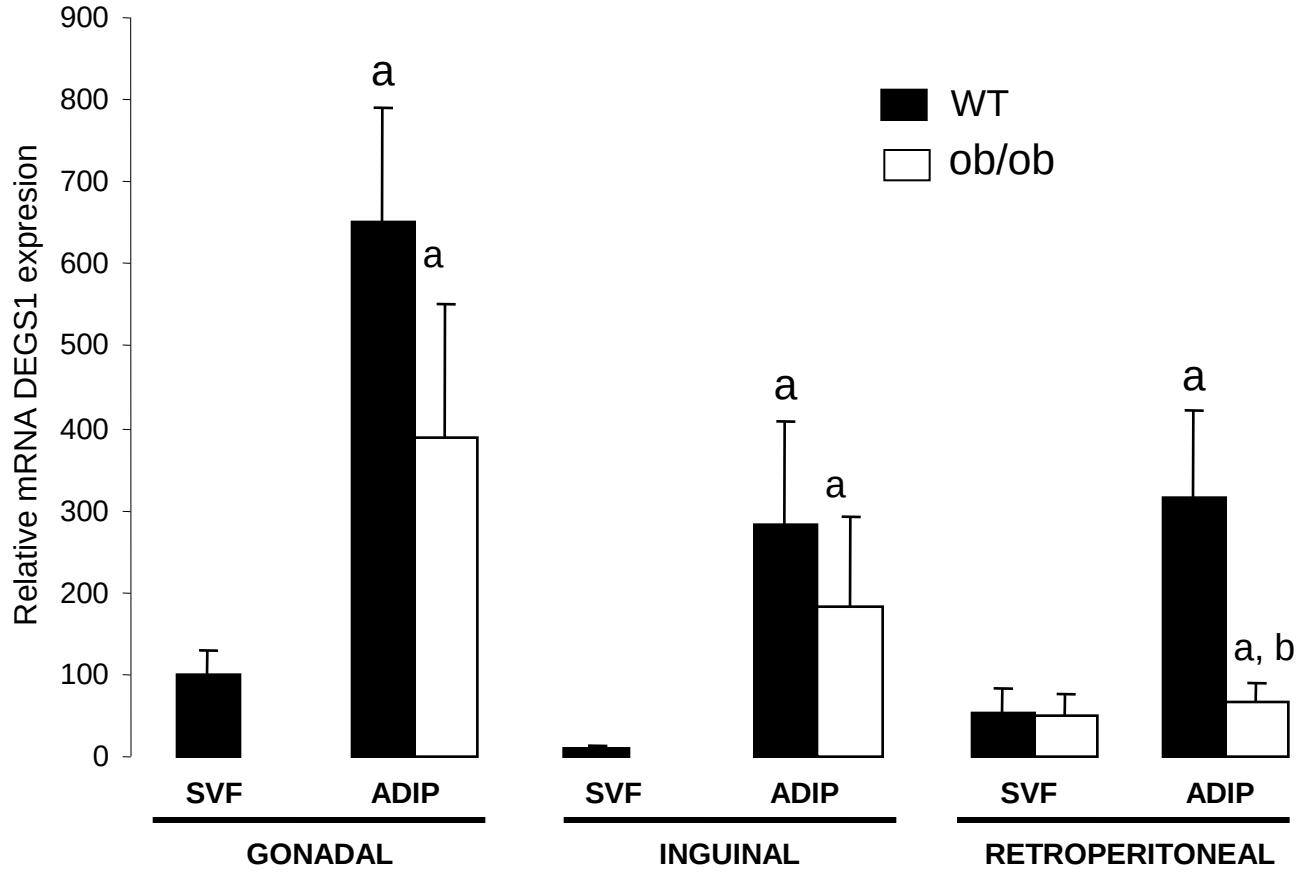

Supplemental Figure 1

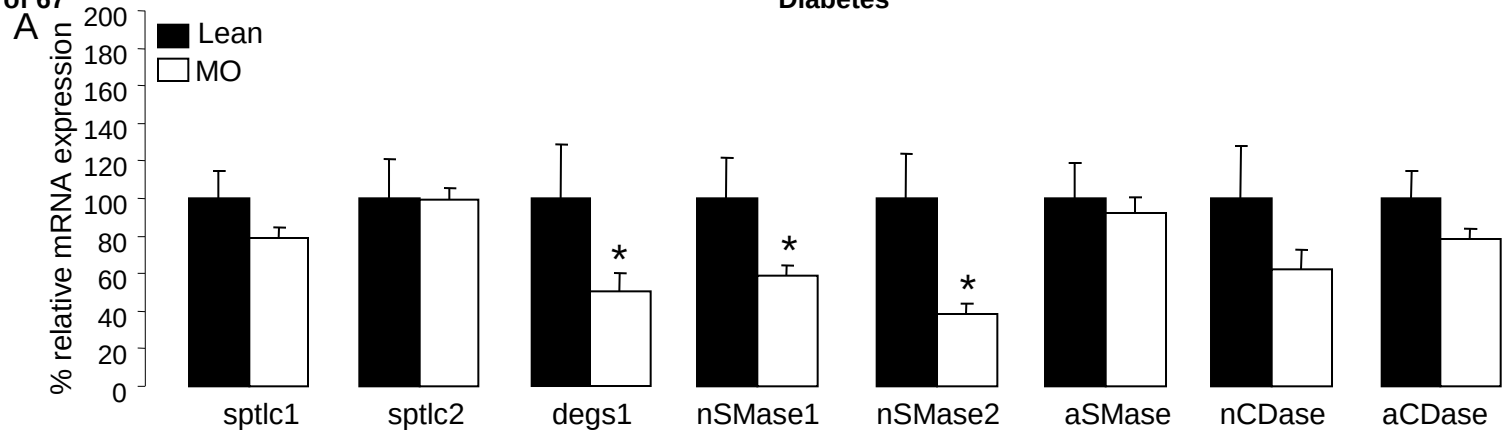

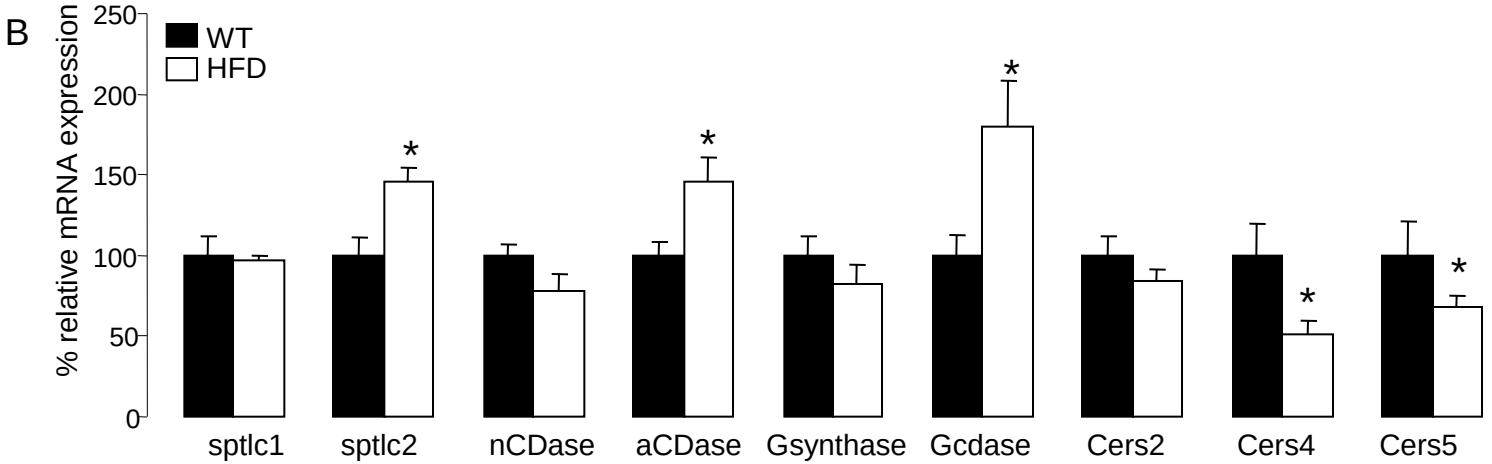

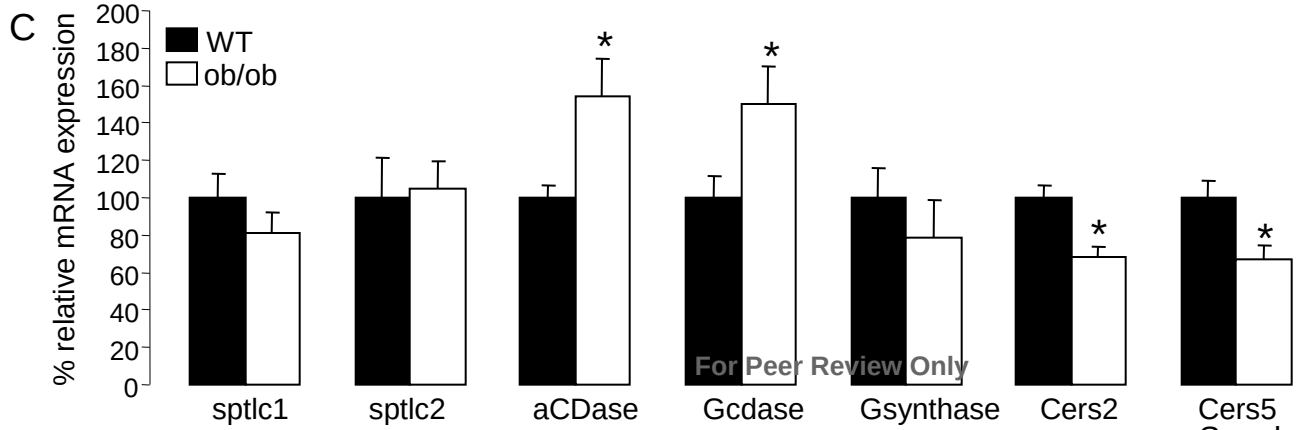

Supplemental Figure 2

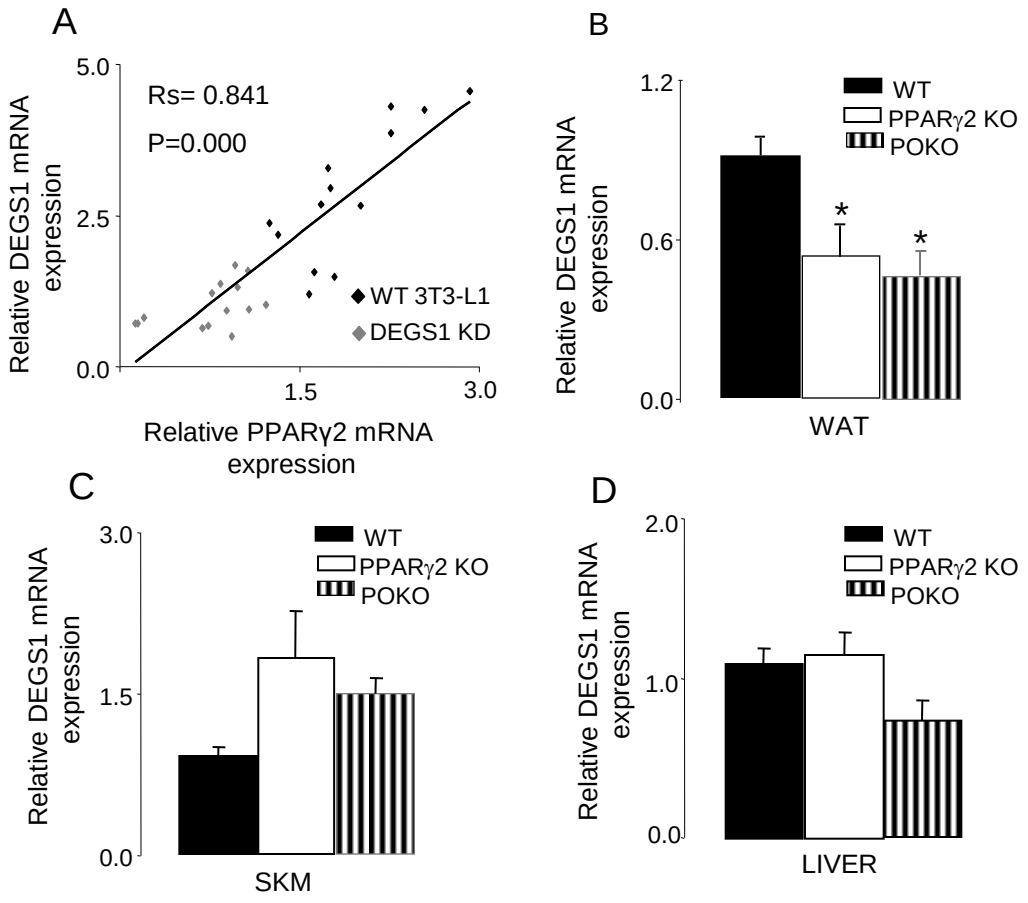

Supplemental Figure 3

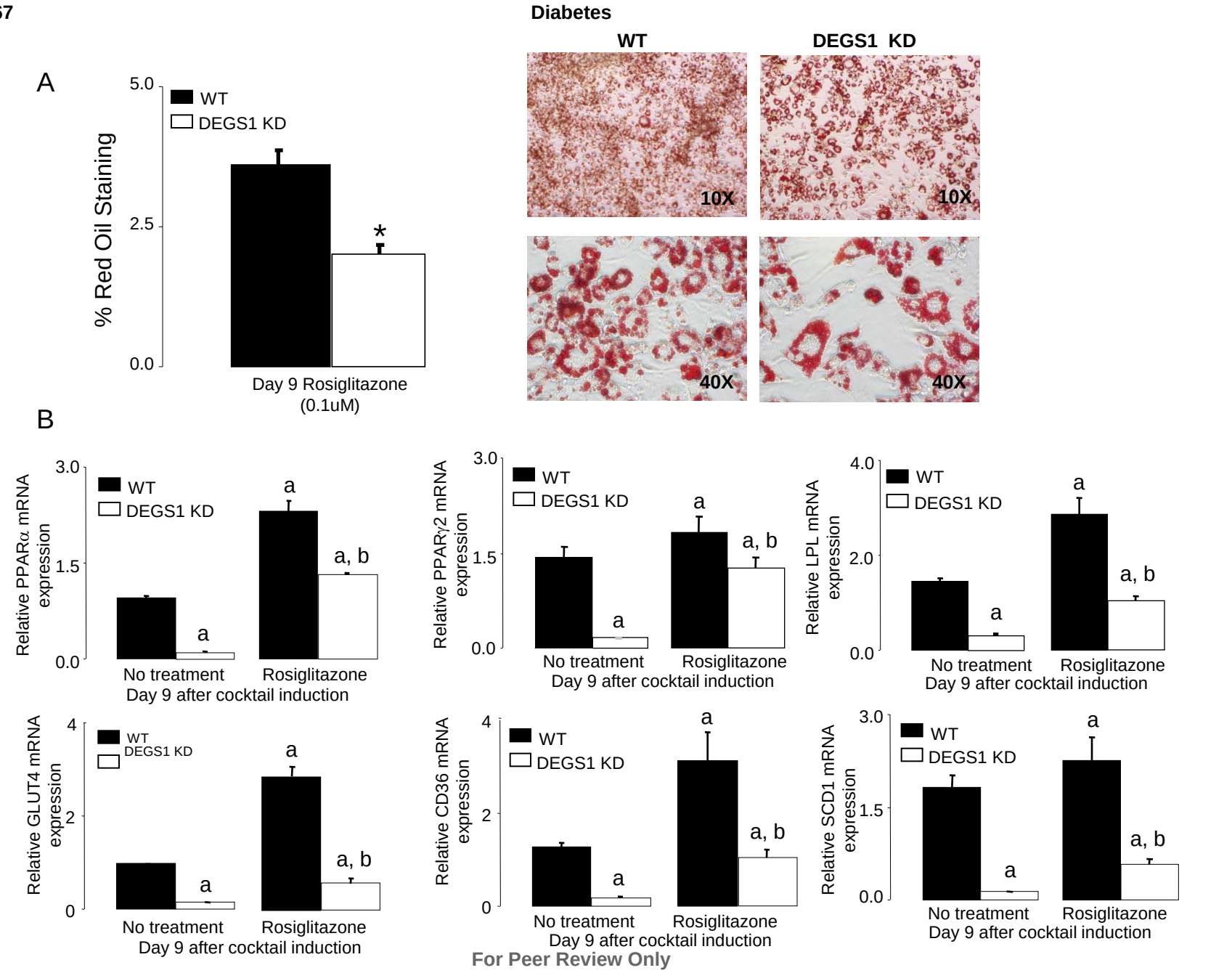

Supplemental Figure 4

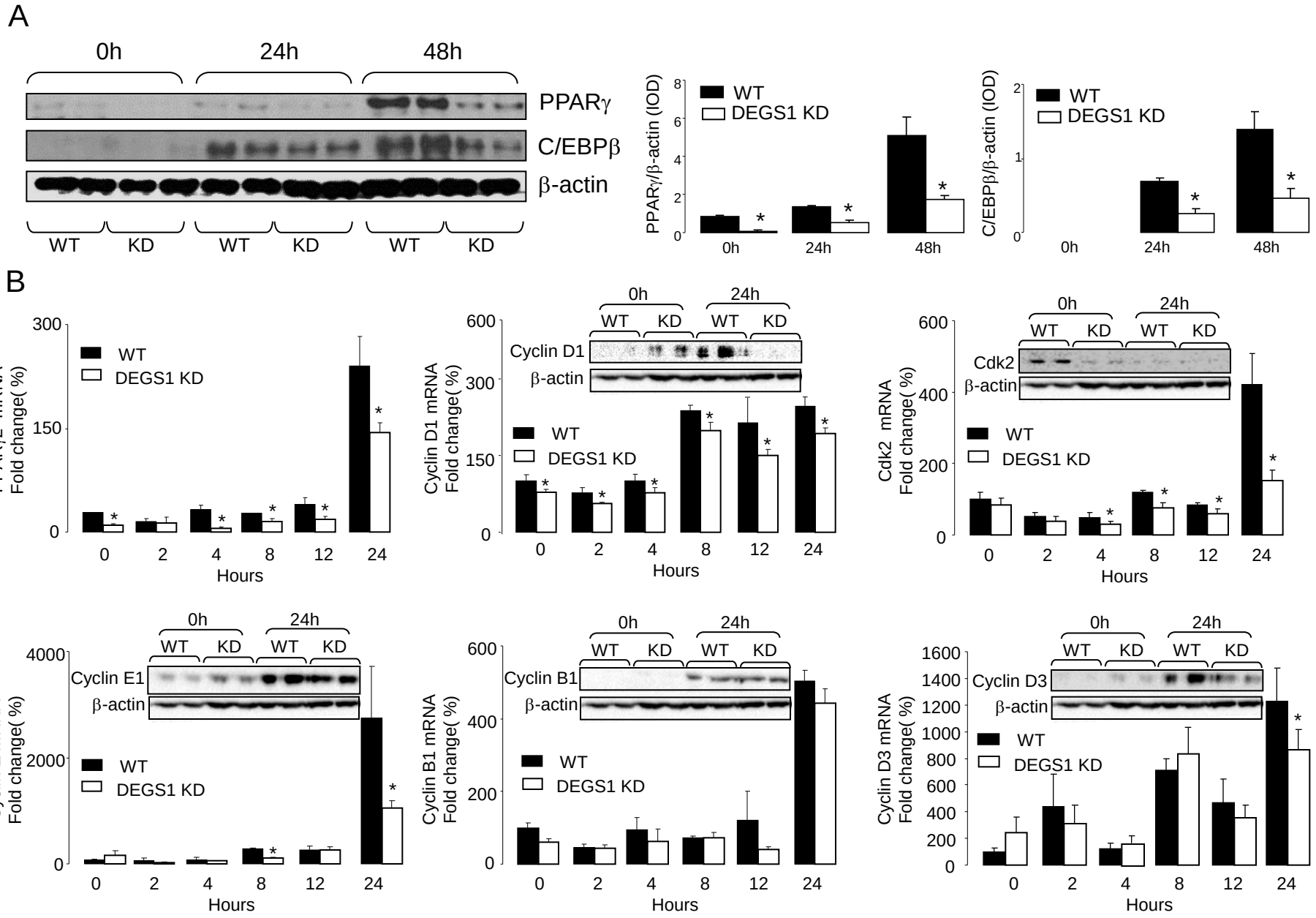

Supplemental Figure 5

A

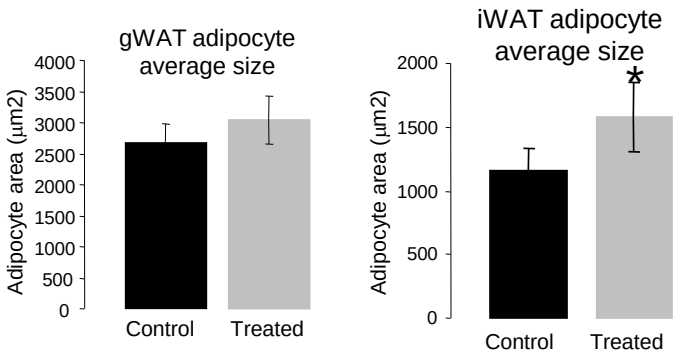

B

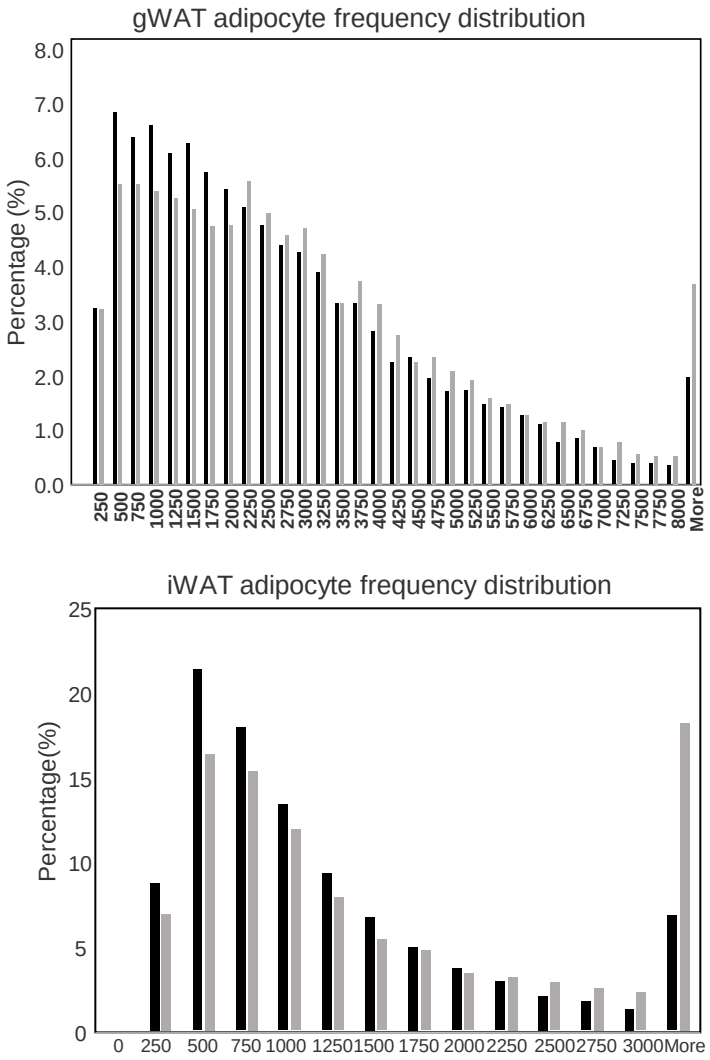

Supplemental figure 6

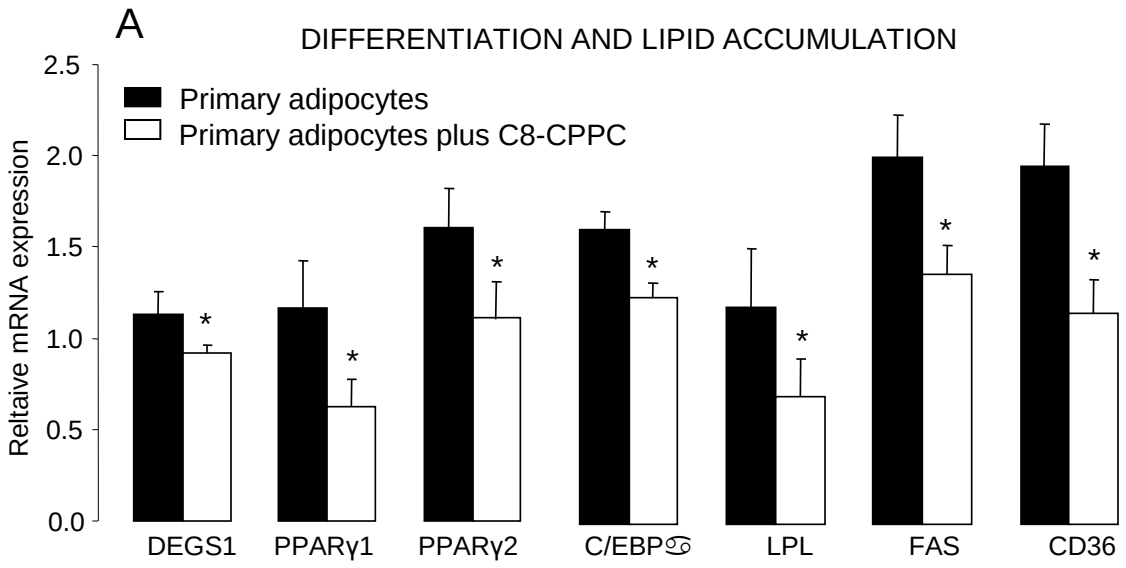

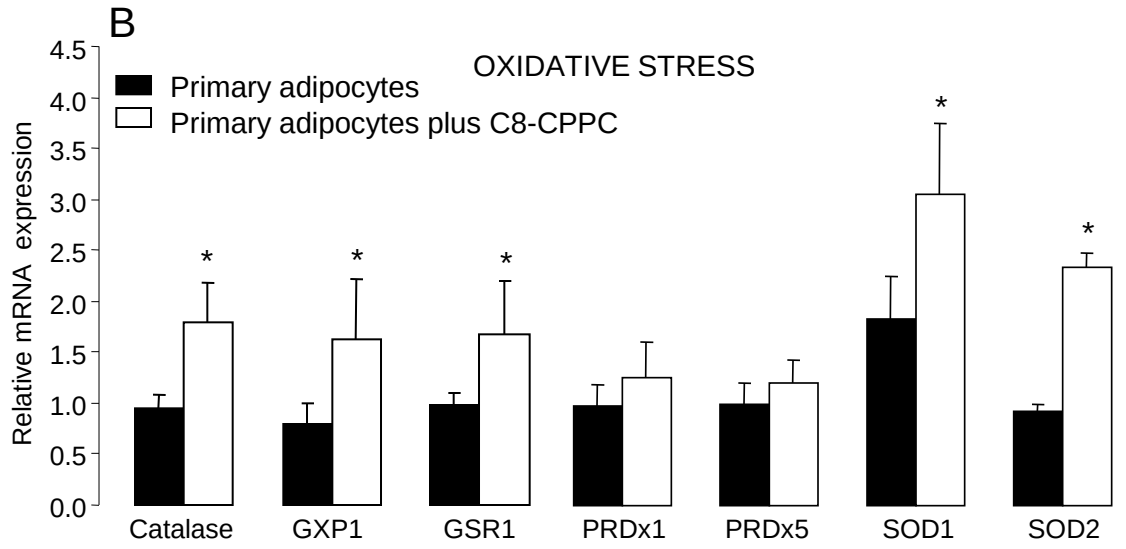

Supplemental Figure 7

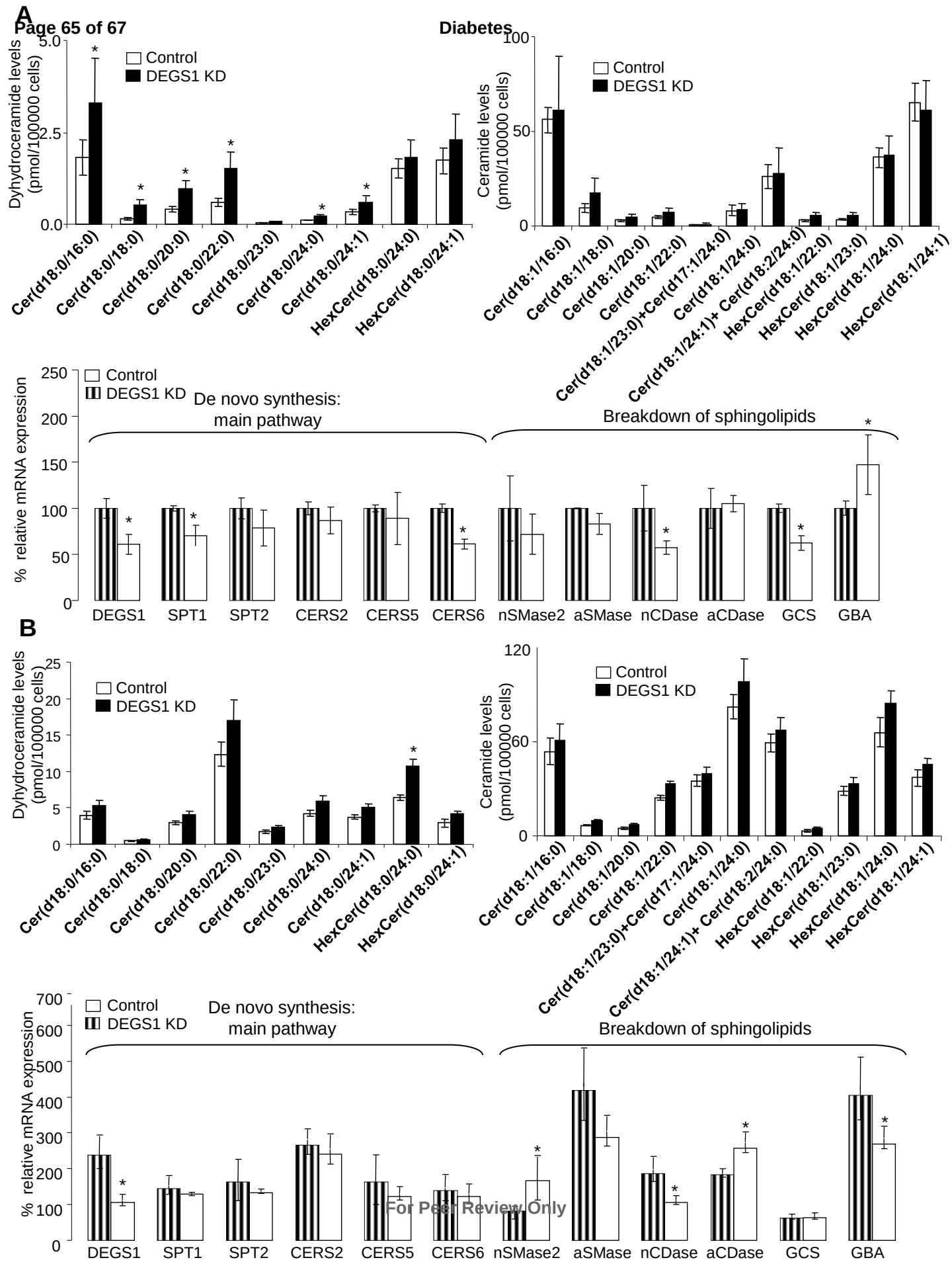

SUPPLEMENTAL FIG.1. mRNA expression levels of DEGS1 in stromal vascular fraction and adipocytes of different fat depots in wild type and ob/ob mice (n=3). $p<0.05$: (a) versus svf. (b) versus lean WT

SUPPLEMENTAL FIG.2. (A) Expression levels of DEGS1 and other ceramide related enzymes in visceral adipose tissue of morbidly obese patients (B) Expression levels ceramide related genes in response to HFD intervention in rodents(C) Expression levels ceramide related genes in ob/ob mice. The panels show means ± SEM of 28 morbidly obese patients and 6 lean controls for the human study and 6 to 8 animals per group in the rodent studies. Significant differences at $p<0.05$: (*) versus lean controls.

SUPPLEMENTAL FIG.3. (A) Positive correlation between the mRNA expression levels of PPARγ2 and DEGS1 in WT and DEGS1 3T3-L1 knockdown cells with or without Rosiglitazone (0.1 μM) at 9 days of adipocyte differentiation. The Spearman correlation coefficients were calculated to estimate the linear correlations between variables. The rejection level for a null hypothesis was $p < 0.01$ (B, C and D) mRNA DESG1 expression in white adipose tissue (WAT), skeletal muscle (SKM) and liver of wild-type, PPARγ2 KO and POKO (PPARγ2 -/- and lep -/-) mice. Graphs show the mean ± SEM of a group of 6-8 animals. *$p< 0.05$ versus wild-type mice.

SUPPLEMENTAL FIG.4. (A) Lipid accumulation in control and DEGS1 3T3-L1 knockdown cells treated with Rosiglitazone (0.1 μM) after 9 days of adipocyte differentiation. Lipid content was analyzed using O Red Oil staining. Graph shows the mean ± SEM of two separate experiments performed in triplicate; *$p< 0.05$ versus control cells. Panels show one representative experiment (B) mRNA expression of genes involved in adipocyte differentiation and lipid accumulation in controls and DEGS1 3T3-L1 knockdown cells with or without Rosiglitazone (0.1 μM) at day 9 of adipocyte differentiation. Graphs show the mean ± SEM of two separate experiments performed in triplicate; $^{a}p< 0.05$ versus WT untreated cells and $^{b}p< 0.05$ versus WT cells treated with Rosiglitazone.

SUPPLEMENTAL FIG.5. (A and B) mRNA and protein expression of PPARγ2, cEBPα, several cyclins and cdk2 in control and DEGS1 knock-down cells during early adipogenesis (at 0, 24 and 48 hours after adipocyte differentiation induction). Panels

show one representative experiment of three different experiments performed separately. Graphs show the mean ± SEM of three separate experiments. *p< 0.05 vs. control cells. Rosi, Rosiglitazone

SUPPLEMENTAL FIG.6.

A) Adipocyte mean area and B) frequency of distribution of gonadal and inguinal WAT adipocytes (1000-3000 per mouse, n=8) from vehicle and C8-CPPC treated mice. $P < 0.05$

SUPPLEMENTAL FIG.7

(A and B) mRNA expression levels of DEGS1, genes involved in differentiation (PPARγ1, PPARγ2 and cEBPα), lipid accumulation (LPL, FAS and CD36) and oxidative stress (Catalase, GXP1, GRS1, PRDx1, PRDx5, SOD1 and SOD2) in primary murine adipocytes treated with C8-CPPC for 20 hours. Panel shows the mean ± SEM of two separated experiments. *p< 0.05 versus untreated primary adipocytes.

SUPPLEMENTAL FIG.8. Total dihydroceramide and ceramide levels in controls and mRNA expression of enzymes involved in ceramide synthesis pathways in control and DEGS1 knockdown cells at 0 (A) and 9 (B) days of differentiation. Graphs show the mean ± SEM of two separate experiments *p< 0.05 vs. control cells for gene expression and p< 0.00 for lipidomic analysis.